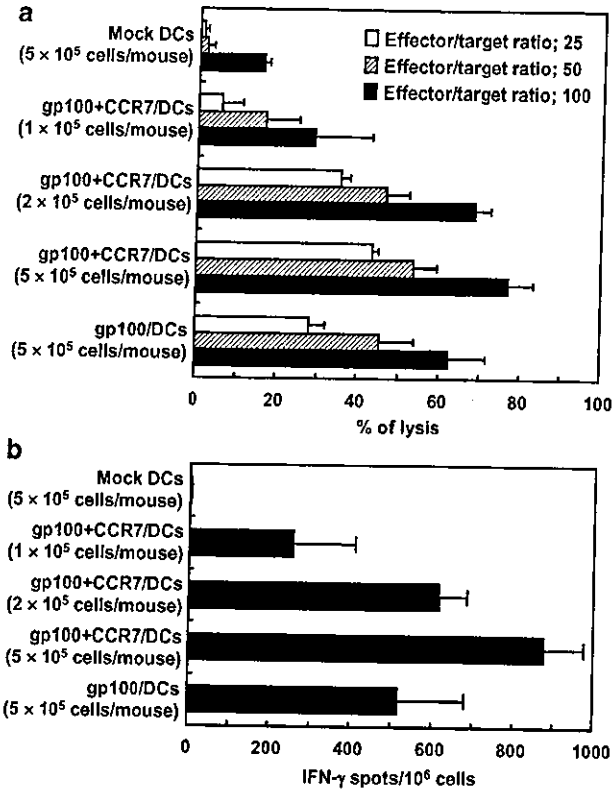

Figure 7 CTL activity and the frequency of IFN-γ-producing cells in splenocytes from mice immunized with DCs cotransduced with CCR7 and gp100 gene by AdRGD. gp100/DCs and gp100+CCR7/DCs were prepared using corresponding vectors at 25 MOI, and then cultured for 24 h. These transduced cells and mock DCs were vaccinated once intradermally into C57BL/6 mice at the indicated cell dosage. At 1 week after immunization, nonadherent splenocytes were prepared from these mice, and then were re-stimulated in vitro for 5 days with IFN-γ-stimulated and MMC-inactivated B16BL6 cells. (a) A cytolytic assay using the re-stimulated splenocytes (effector cells) was performed against IFN-γ-stimulated B16BL6 cells (target cells). The data represent the mean±s.e. of four independent cultures from four individual mice. (b) IFN-γ-producing cells in re-stimulated splenocytes were evaluated by mouse IFN-γ ELISPOT assay. The data represent the mean±s.d. of results from four mice.

efficient priming and subsequent activation of antitumor CTLs requires the processing and presentation of TAAs as peptide fragments in the context of appropriate MHC class I molecules by APCs.[15] DCs are the most potent APCs and are uniquely capable of presenting novel antigens to naive T cells to initiate and modulate immune responses.[5–7] Owing to these properties, TAA-loaded DCs are considered promising vaccine carriers in immune intervention strategies against cancer. However, very few DCs in currently available DC-based immunotherapies are capable of migrating from an administration site to regional lymphoid tissue,[16–18] where they present MHC class I- and II-restricted peptides to naive T cells, because optimal DC conditioning for enhancing migratory ability is not yet established. Therefore, increasing the migratory ability of a DC vaccine toward lymphoid tissues would remarkably improve the efficacy of DC-based immunotherapy because priming/activation of immune effector cells would be significantly promoted. In the present study, we focused on the chemokine receptor, CCR7, which manages facilitated DC migration to lymphoid tissues, and attempted to create a DC vaccine that sufficiently expressed CCR7 on the surface by gene transduction.

A vector system that can effectively deliver a foreign gene to DCs is essential for preparing a genetically modified-DC vaccine. We have demonstrated that AdRGD can enhance gene transduction efficiency against murine and human DCs as compared with conventional Ad because of the expression of the RGD sequence, the αv-integrin-targeting peptide, at the HI loop in the fiber knob.[11–14] Therefore, we constructed AdRGD-CCR7, which carried the expression cassette containing mouse CCR7 cDNA under the control of the cytomegalovirus promoter, and confirmed the vector's performance. RT-PCR analysis indicated that transfection using AdRGD-CCR7 allowed murine bone marrow-derived DCs to express abundant CCR7 mRNA, and CCR7 mRNA expression in CCR7/DCs was the highest at 24 h after gene transduction. Furthermore, CCR7/DCs cultured for 24 h exhibited sufficient CCR7 protein expression on the cell surface in flow cytometric analysis and demonstrated strong migratory ability toward CCL21, a CCR7 ligand secreted constitutively from lymphoid tissues, depending on both CCL21 concentration in a 4 h chemotaxis assay and AdRGD-CCR7 dose in transfection. That is, efficient CCR7-gene transduction into DCs by AdRGD reinforced surface expression of CCR7, which sensed a CCL21 concentration gradient and transmitted intracellular signals associated with migration in their original biologically active form. Although DCs generally enhance the expression of CCR7 and acquire migratory ability to lymphoid tissues by various maturation stimuli, an increase in CCR7 mRNA levels and enhancement of migratory activity toward CCL21 were not observed in LPS/DCs, contrary to our expectation. Granucci *et al*[19] reported that DCs stimulated with LPS significantly decreased their intrinsic migratory ability and increased the antigen uptake function at 1–2 h post-stimulation. This phenomenon probably represents the *in vivo* stage during which DCs remain at an inflammation site caused by the components of invading bacteria, such as LPS, and capture antigens by full endocytosis. In addition, Granucci *et al*[19] demonstrated that, at around 4 h after LPS activation, DCs recovered their migratory ability and started to progressively lose antigen uptake function until they reached the mature stage in which LPS/DCs showed poor antigen uptake and migratory activity. Therefore, because in the present study we tested the responses 24 h after LPS stimulation, low CCR7 mRNA levels and poor migratory response to CCL21 by LPS/DCs may have been observed because tests were run after the optimal time point, suggesting that the control of DC-migratory activity by LPS stimulation is difficult.

DCs are strong initiators of defense mechanisms that combat infectious diseases and cancer, but, in their role as APCs, DCs are also involved in immune suppression and immune tolerance.[20–23] In their induction of a positive immune response, immature DCs capture invading antigens at peripheral locations and are then activated by inflammatory stimuli, such as interleukin (IL)-1β, tumor necrosis factor-α, and bacterial components, to migrate to T-cell-rich areas in regional LN. In these processes, DCs enhance the expression of MHC/costimulatory molecules, which is essential for T-cell surface sensitization for effective induction of T-cell-

dependent primary immune responses. On the other hand, in negative immune regulation, immature DCs take up resident biological materials or apoptotic bodies and present processing peptides without acquiring activated phenotypes during migration to regional LN.[24,25] Therefore, a full analysis and understanding of immunological characteristics of DC vaccine is imperative for the development of DC-based immunotherapy because the polarity of the immune response is greatly influenced by the activated state of DCs during T-cell sensitization. CCR7/DCs created in the present study maintained inherent endocytotic activity, suggesting that CCR7/DCs administered into tumor tissue can capture necrotic or apoptotic tumor cell fragments and may induce TAA-specific immune responses. Yanagawa *et al*[26] reported that internalization of FITC-dextran in murine mature DCs increased in the presence of CCR7 ligand, CCL19 or CCL21. These results support the notion that CCL21, secreted from lymphatic vessels located near a tumor, may encourage uptake of tumor cell fragments by CCR7/DCs injected into the tumor tissue. Although high endocytotic activity is a characteristic feature of immature DCs, flow cytometric analysis indicated that CCR7/DCs enhanced expression of MHC/costimulatory molecules and allo-MLR suggested the reinforcement of T-cell proliferation-stimulating ability. These results agreed with our previous report demonstrating that transduction using AdRGD could enhance the maturation status of DCs,[13] strongly suggesting that CCR7 gene transduction using AdRGD did not inhibit the original APC characteristics of DCs and that CCR7/DCs can function as a useful vaccine possessing sufficient T-cell activation ability *in vivo*.

Although a technique to label DCs with radioisotopes or fluorescent substances is frequently used for evaluating *in vivo* kinetics of administered DC vaccines,[27–32] release via exosomes or leakage of the labeling material from DCs complicates the analysis. Eggert *et al*[33] reported that application of EGFP-Tg mouse-derived DCs avoided this problem and enabled simple evaluation and analysis of the kinetics of administered DCs without the need for labeling. Thus, we investigated the migratory ability of CCR7/DCs by flow cytometric analysis of regional LN cells prepared from mice intradermally injected with transduced EGFP-Tg mouse-derived DCs. At 48 h post-injection, regional LNs that served as administration sites for CCR7/DCs were obviously larger than contralateral LNs under macroscopic observation, and the frequency of $EGFP^+CD11c^+$ DCs in regional LN cells was 1.93 ± 0.54, 0.57 ± 0.19, and $0.12\pm0.04\%$ (mean$\pm$s.e.) for CCR7/DCs-, Luc/DCs-, and mock DCs-injected mice, respectively. In addition, we could prepare more cells from regional LN in CCR7/DCs-injected mice than from the Luc/DC or mock DC groups, suggesting that not only administered DCs but also other immune cells, such as T cells, might accumulate in regional LN in mice injected with CCR7/DCs.

Previously, we demonstrated that immunization with DCs efficiently transduced with gp100 gene by AdRGD could significantly inhibit the growth and lung metastasis of murine B16BL6 melanoma *in vivo*.[14] In order to actually evaluate the predominancy of CCR7-transduced DCs as a vaccine carrier *in vivo*, we investigated anti-B16BL6 melanoma effects in mice vaccinated with DCs genetically engineered to simultaneously express gp100 and CCR7. Although antigen presentation via MHC class I molecules in the experiment using AdRGD-OVA was the same for DCs transduced with OVA gene alone and co-transduced with OVA and CCR7 gene, immunization with gp100+CCR7/DCs could more effectively suppress growth of B16BL6 tumors than vaccination with gp100/DCs. Furthermore, DC vaccine co-transduced with the TAA gene and the CCR7 gene effectively induced TAA-specific and IFN-γ-producing CTLs using a lower dosage than conventional DC vaccine transduced with TAA gene alone. These data suggest that augmentation of lymphoid tissue directivity of DCs by efficient CCR7-gene transduction can reduce the DC vaccine dosage that is needed to elicit efficacious therapeutic effects in DC-based immunotherapy. In other words, this method may considerably reduce the cost, time, and effort for DC vaccine preparation and relieve the patient from the burden of frequent blood drawing for DC isolation.

In conclusion, our data strongly suggested that *in vivo* kinetic control of DC vaccine, namely the establishment of an active DC delivery system to lymphoid tissues, was very useful for improving the efficacy of DC-based immunotherapy. We expect that superior lymphoid tissue accumulation of DCs transduced with the CCR7 gene is advantageous for a vaccine carrier because of efficient activation of immune effector cells in regional LNs and a rapid supply of activated effector cells to the whole body. Recently, optimized DC conditioning, which includes stimulation of antigen-presenting DCs with various cytokines or ligand molecules, has been investigated for the development of more effective DC-based immunotherapy. Several reports demonstrated that DC stimulation by prostaglandin E_2[34–36] or the pre-induction of inflammatory response at the DC-administration site[37] was effective in promoting migration of administered DCs to lymphoid tissues. Further research and development of 'lymphoid tissue-directivity DC' vaccine based on these data and our results may greatly improve efficacy and lead to clinical application of DC-based immunotherapy.

Materials and methods

Cell lines and mice

A murine B16BL6 melanoma cell line ($H\text{-}2^b$) was cultured in minimum essential medium supplemented with 7.5% fetal bovine serum (FBS) and antibiotics. The helper cell line, 293 cells, was grown in Dulbecco's modified Eagle medium supplemented with 10% FBS and antibiotics. CD8-OVA 1.3 cells,[38] specific T–T hybridoma against OVA^+ $H\text{-}2K^b$ (kindly provided by Dr CV Harding; Department of Pathology, Case Western Reserve University, Cleveland, OH, USA), were maintained in Dulbecco's modified Eagle medium supplemented with 10% FBS, 50 μM 2-mercaptoethanol, and antibiotics. Female C57BL/6 mice ($H\text{-}2^b$) and female BALB/*c* mice ($H\text{-}2^d$), aged 7–8 weeks, were purchased from SLC Inc. (Hamamatsu, Japan). EGFP-Tg mice, C57BL/6 TgN(act-EGFP)OsbC14-Y01-FM131,[39] were kindly provided by Dr M Okabe (Genome Information Research Center, Osaka University, Suita, Japan). All mice were held under specific pathogen-free conditions and the experimental procedures were in accordance with the Osaka University guidelines for the welfare of animals in experimental neoplasia.

Vectors

Replication-deficient AdRGD was based on the adenovirus serotype 5 backbone with deletions of E1 and E3 regions. The RGD sequence for αv-integrin targeting was inserted into the HI loop of the fiber knob using a two-step method as described previously.[40] The expression cassette containing mouse CCR7 cDNA derived from pBluescript SK(+)/mCCR7 under the control of the cytomegalovirus promoter was inserted into the E1-deletion site to construct AdRGD-CCR7, using an improved *in vitro* ligation method as described previously.[40–42] Luciferase-expressing AdRGD (AdRGD-Luc), OVA-expressing AdRGD (AdRGD-OVA), and gp100-expressing AdRGD (AdRGD-gp100) were constructed previously.[12–14] All recombinant AdRGDs were propagated in 293 cells, purified by two rounds of cesium chloride gradient ultracentrifugation, dialyzed, and stored at −80°C. Titers of infective AdRGD particles were evaluated by the end-point dilution method using 293 cells.

Mouse bone marrow-derived DCs

DCs were prepared according to the method of Lutz *et al*,[43] with slight modification. Briefly, bone marrow cells flushed from the femurs and tibias of C57BL/6 or EGFP-Tg mice were seeded at 5×10^6 cells per sterile 100-mm bacterial grade culture dish in 10 ml of RPMI 1640 containing 10% FBS, 40 ng/ml recombinant murine granulocyte/macrophage colony-stimulating factor (GM-CSF; kindly provided by KIRIN Brewery Co., Ltd, Tokyo, Japan), 50 μM 2-mercaptoethanol, and antibiotics. On day 3, another 10 ml of culture medium was added to the dish for medium replenishment. On day 6, 10 ml of the culture supernatant was collected and centrifuged at 1500 rpm for 5 min at room temperature, and the pellet was resuspended in 10 ml of fresh culture medium, and then returned to the original dish to conserve unattached cells. Eight-day-old DCs (nonadherent cells) were harvested and used as intact immature DCs in subsequent experiments. DCs cultured for another 24 h with media containing 1 μg/ml LPS (Nacalai Tesque, Inc., Kyoto, Japan) were used as phenotypically mature DCs.

Viral transduction into DCs

DCs were suspended at a concentration of 5×10^6 cells/ml in FBS-free RPMI 1640 and placed in a 15-ml conical tube. Each AdRGD was added at various MOI, the suspension was mixed well, and the tube was incubated at 37°C for 2 h with occasional gentle agitation. The cells were washed three times with phosphate-buffered saline (PBS) and resuspended in a suitable solution.

Semiquantitative RT-PCR analysis

CCR7/DCs, Luc/DCs, and mock DCs were cultured on 100-mm bacterial grade culture dishes in GM-CSF-free culture medium. Mouse CCR7 gene expression was assessed by semiquantitative RT-PCR analysis as follows. Total RNA was isolated from these cells and LPS/DCs using Sepasol-RNA I Super (Nacalai Tesque, Inc.) according to the manufacturer's instructions, and then RT proceeded for 60 min at 42°C in a 50 μl reaction mixture containing 5 μg total RNA treated with DNase I, 10 μl 5 × RT buffer, 5 mM $MgCl_2$, 1 mM dNTP mix, 1 μM random primer (9-mer), 1 μM oligo$(dT)_{20}$, and 100 U ReverTra Ace (TOYOBO Co., Ltd, Osaka, Japan). PCR amplification of the CCR7 and β-actin transcripts was performed in 50 μl of a reaction mixture containing 1 μl of RT material, 5 μl 10 × PCR buffer, 1.25 U *Taq* DNA polymerase (TOYOBO Co., Ltd), 1.5 mM $MgCl_2$, 0.2 mM dNTP, and 0.4 μM primers. The sequences of the specific primers were as follows; mouse CCR7: forward, 5′-aca gcg gcc tcc aga aga aca gcg g-3′; reverse, 5′-tga cgt cat agg caa tgt tga gct g-3′; mouse β-actin: forward, 5′-tgt gat ggt ggg aat ggg tca g-3′; reverse, 5′-ttt gat gtc acg cac gat ttc c-3′. After denaturation for 2 min at 95°C, 20 cycles of denaturation for 30 s at 95°C, annealing for 30 s at 60°C, and extension for 30 s at 72°C were repeated and followed by completion for 4 min at 72°C. The PCR product was electrophoresed through a 3% agarose gel, stained with ethidium bromide, and visualized under UV radiation. The expected PCR product sizes were 345 bp (CCR7) and 514 bp (β-actin). Quantification of PCR products was performed by densitometry analysis, and the relative CCR7 mRNA expression level was calculated as the ratio of the densitometric units of CCR7 PCR-products to the densitometric units of β-actin PCR products.

Flow cytometric analysis for mouse CCR7

CCR7/DCs and Luc/DCs were prepared by using corresponding vectors at 50 MOI. These transduced DCs, LPS/DCs, and mock DCs were cultured on 100-mm bacterial grade culture dishes in GM-CSF-free culture medium for 24 h. The cells (1×10^6) were fixed by incubation for 10 min in 2% paraformaldehyde, and then incubated with 100 μl staining buffer (PBS containing 0.1% bovine serum albumin and 0.01% NaN_3) containing the anti-FcγRII/III monoclonal antibody (2.4G2; rat $IgG_{2b,\kappa}$; BD Biosciences, San Jose, CA, USA) to block nonspecific binding of the subsequently used antibody reagents. After 1 h, the cells were incubated overnight with anti-mouse CCR7 polyclonal antibody (goat Ig; ImmunoDetect Inc., Fayetteville, NY, USA) at a 1:10 dilution. Successively, cells were incubated for 2 h with FITC-conjugated rabbit anti-goat Ig (DakoCytomation, Kyoto, Japan) at a 1:100 dilution. Finally, 30 000 events of the stained cells were analyzed for mouse CCR7 protein expression by a FACSCalibur flow cytometer using CellQuest software (Becton Dickinson, Tokyo, Japan). Between all incubation steps, cells were washed three times with staining buffer.

In vitro chemotaxis assay

CCR7/DCs, Luc/DCs, and mock DCs were cultured for 24 or 48 h in GM-CSF-free medium. Chemotactic activity of these DCs and LPS/DCs for CCL21 was measured by an *in vitro* chemotaxis assay across a polycarbonate membrane with 5-μm pores (Chemotaxicell-24; Kurabo Industries Ltd, Osaka, Japan). Recombinant murine CCL21 (PeproTech EC Ltd, London, England) dissolved in an assay medium (RPMI 1640 containing 0.5% bovine serum albumin and 20 mM HEPES) was added to a 24-well culture plate. DCs were suspended with the assay medium and were placed in a Chemotaxicell-24 installed on each well at 10^6 cells. Cell migration was allowed for 4 h at 37°C in a 5% CO_2 atmosphere. Cells that migrated into the lower compartment were counted using a NucleoCounter™ (ChemoMetec, Allerød, Denmark), and the chemotactic activity was expressed in terms of

the percentage of the input cells calculated by the following formula: (% of input cells) = (the number of migrated cells)/(the number of cells placed in Chemotaxicell-24; 10^6 cells) × 100.

Analysis of surface marker expression

All immunoreagents used in this experiment were purchased from BD Biosciences. CCR7/DCs and Luc/DCs were prepared by using corresponding vectors at 50 MOI. At 24 h after transduction, immunophenotype of transduced DCs, LPS/DCs, and mock DCs was confirmed by flow cytometric analysis. Briefly, 10^6 cells in 100 µl staining buffer were incubated for 30 min on ice with the 2.4G2 monoclonal antibody to block nonspecific binding of the subsequently used immunoreagents. The cells were resuspended in 100 µl staining buffer and incubated for 30 min on ice using the manufacturer's recommended amounts of biotinylated monoclonal antibodies: 28-8-6 (anti-H-2K^b/D^b), AF6-120.1 (anti-I-A^b), 3/23 (anti-CD40), 3E2 (anti-CD54), 16-10A1 (anti-CD80), and GL1 (anti-CD86). The cells were then resuspended in 100 µl staining buffer containing phycoerythrin-conjugated streptavidin at a 1:200 dilution, and nonspecific binding was measured using phycoerythrin-conjugated streptavidin alone. After incubation for 30 min on ice, 30 000 events of the stained cells were analyzed for surface phenotype by flow cytometry. Between all incubation steps, cells were washed three times with staining buffer.

Allogenic MLR

C57BL/6 DCs were transduced with AdRGD-CCR7 or AdRGD-Luc at 50 MOI, and then cultured for 24 h. Allogenic naive T cells were purified from BALB/*c* splenocytes as nylon wool nonadherent cells, and were used as responder cells at 1×10^5 cells/well in 96-well plates. CCR7/DCs, Luc/DCs, LPS/DCs, or mock DCs (stimulator cells) were inactivated by 50 µg/ml mitomycin C (MMC) for 30 min and added to responder cells in varying cell numbers. Cells were co-cultured in 100 µl RPMI 1640 supplemented with 10% FBS, 50 µM 2-mercaptoethanol, and antibiotics at 37°C and 5% CO_2 for 3 days. Control wells contained either stimulator cells alone or responder cells alone. Cell cultures were pulsed with 5-bromo-2′-deoxyuridine (BrdU) during the last 18 h, and then proliferation of responder cells was evaluated by Cell Proliferation ELISA, BrdU (Roche Diagnostics Co., Indianapolis, IN, USA).

Antigen uptake assay

CCR7/DCs and Luc/DCs were prepared by using corresponding vectors at 50 MOI. These cells, LPS/DCs, and mock DCs were cultured for 24 h, and then resuspended at 5×10^6 cells/ml in ice-cold PBS containing 1 mg/ml FITC-dextran (MW: 77 000; Sigma Chemical Co., St Louis, MO, USA). The cells were incubated at 37 or 4°C to determine background uptake. After 1 h, the cells were washed extensively with ice-cold PBS and analyzed by flow cytometry.

In vivo migration assay

EGFP-Tg mouse-derived DCs were transduced with AdRGD-CCR7 or AdRGD-Luc at 50 MOI, and then cultured for 24 h. These transduced cells and mock DCs were intradermally injected into the left flank of wild-type C57BL/6 mice at 2×10^6 cells/50 µl. After 2 days, the draining inguinal LNs were collected from these mice, and then a single-cell suspension was prepared. The isolated LN cells were blocked by 2.4G2 monoclonal antibody and stained by indirect immunofluorescence with biotinylated anti-CD11c monoclonal antibody (HL3; BD Biosciences) and PerCP-conjugated streptavidin. The stained cells were analyzed by flow cytometry acquiring 500 000 events, and the number of migrated DCs into draining LNs was calculated by multiplying the EGFP$^+$CD11c$^+$ cell frequency by the total number of isolated LN cells.

Antigen-presentation assay

C57BL/6 DCs were transduced with various combinations of AdRGD-OVA, AdRGD-CCR7, and AdRGD-Luc each at 25 MOI, and then seeded on a 96-well flat-bottom culture plate at a density of 1×10^5 cells/well. These cells were co-cultured with 1×10^5 cells/well CD8-OVA 1.3 cells at 37°C for 20 h. The response of stimulated CD8-OVA 1.3 cells was assessed by determining the amount of IL-2 released into an aliquot of culture medium (100 µl) using a murine IL-2 ELISA KIT (Biosource International, Camarillo, CA, USA). Relative OVA-presentation level via MHC class I molecules in each transduced DC was calculated by the following formula: (relative OVA-presentation level) = (IL-2 level in tested group)/(IL-2 level in group using DCs transduced with AdRGD-OVA alone) × 100.

Tumor protection assay

DCs were transduced with AdRGD-CCR7 alone, AdRGD-gp100 alone, or a combination of AdRGD-CCR7 and AdRGD-gp100, each at 25 MOI, and then cultured for 24 h. These transduced DCs and mock DCs were intradermally injected into the left flank of C57BL/6 mice at 2 or 5×10^5 cells/50 µl. At 1 week after the vaccination, 4×10^5 B16BL6 melanoma cells were intradermally inoculated into the right flank of the mice. The major and minor axes of the tumor were measured using microcalipers, and the tumor volume was calculated by the following formula: (tumor volume; mm^3) = (major axis; mm) × (minor axis; mm)^2 × 0.5236. The mice were euthanized when one of the two measurements was greater than 20 mm.

Eu-release assay and ELISPOT assay for B16BL6-specific CTLs

DCs were transduced with AdRGD-gp100 alone or a combination of AdRGD-CCR7 and AdRGD-gp100 at 25 MOI, and then cultured for 24 h. These transduced DCs and mock DCs were administered once intradermally into the left flank of C57BL/6 mice at 1, 2, or 5×10^5 cells/50 µl. At 1 week after immunization, nonadherent splenocytes were prepared from these mice and re-stimulated *in vitro* using B16BL6 cells, which were cultured in media containing 100 U/ml recombinant murine IFN-γ (PeproTech EC Ltd) for 24 h and inactivated with 50 µg/ml MMC at 37°C for 30 min, at an effector/stimulator ratio of 10 in RPMI 1640 supplemented with 10% FBS, 50 µM 2-mercaptoethanol, and antibiotics. After 5 days, the splenocytes were collected and used as CTL effector cells. Target cells, IFN-γ-stimulated B16BL6 cells, were Eu-labeled and a Eu-release assay

was performed as described previously.[44] Cytolytic activity was determined using the following formula: (% of lysis) = ((experimental Eu release−spontaneous Eu release)/(maximum Eu release−spontaneous Eu release)) × 100. Spontaneous Eu release of the target cells was <10% of maximum Eu release by the detergent. In addition, IFN-γ-producing cells in the re-stimulated splenocytes were detected by using Mouse IFN-γ ELISPOT Kit (BD Biosciences) according to the manufacturer's instruction. Splenocytes from unimmunized mice had a frequency of three IFN-γ spots/10^6 cells with or without re-stimulation.

Acknowledgements

We are grateful to KIRIN Brewery Co., Ltd (Tokyo, Japan) for providing recombinant murine GM-CSF, to Dr Clifford V Harding (Department of Pathology, Case Western Reserve University, Cleveland, OH, USA) for providing the CD8-OVA 1.3 cells, and to Dr Masaru Okabe (Genome Information Research Center, Osaka University, Suita, Japan) for providing the C57BL/6 TgN(act-EGFP)OsbC14-Y01-FM131 mice. This study was supported in part by the Research on Health Sciences Focusing on Drug Innovation from the Japan Health Sciences Foundation; by a Grant-in-Aid for Young Scientists (16790114) from the Ministry of Education, Culture, Sports, Science and Technology of Japan; by Senri Life Science Foundation; by the Science Research Promotion Fund of the Japan Private School Promotion Foundation; by grants from the Bioventure Development Program of the Ministry of Education, Culture, Sports, Science and Technology of Japan; and by grants from the Ministry of Health, Labour and Welfare in Japan.

References

1 Nestle FO *et al.* Vaccination of melanoma patients with peptide- or tumor lysate-pulsed dendritic cells. *Nat Med* 1998; **4**: 328–332.
2 Thurner B *et al.* Vaccination with Mage-3A1 peptide-pulsed mature, monocyte-derived dendritic cells expands specific cytotoxic T cells and induces regression of some metastases in advanced stage IV melanoma. *J Exp Med* 1999; **190**: 1669–1678.
3 Lodge PA *et al.* Dendritic cell-based immunotherapy of prostate cancer: immune monitoring of a phase II clinical trial. *Cancer Res* 2000; **60**: 829–833.
4 Yu JS *et al.* Vaccination of malignant glioma patients with peptide-pulsed dendritic cells elicits systemic cytotoxicity and intracranial T-cell infiltration. *Cancer Res* 2001; **61**: 842–847.
5 Banchereau J, Steinman RM. Dendritic cells and the control of immunity. *Nature* 1998; **392**: 245–252.
6 Steinman RM *et al.* Antigen capture, processing, and presentation by dendritic cells: recent cell biological studies. *Hum Immunol* 1999; **60**: 562–567.
7 Mellman I, Steinman RM. Dendritic cells: specialized and regulated antigen processing machines. *Cell* 2001; **106**: 255–258.
8 Gunn MD *et al.* Mice lacking expression of secondary lymphoid organ chemokine have defects in lymphocyte homing and dendritic cell localization. *J Exp Med* 1999; **189**: 451–460.
9 Förster R *et al.* CCR7 coordinates the primary immune response by establishing functional microenvironments in secondary lymphoid organs. *Cell* 1999; **99**: 23–33.
10 Arthur JF *et al.* A comparison of gene transfer methods in human dendritic cells. *Cancer Gene Ther* 1997; **4**: 17–25.
11 Okada N *et al.* Efficient gene delivery into dendritic cells by fiber-mutant adenovirus vectors. *Biochem Biophys Res Commun* 2001; **282**: 173–179.
12 Okada N *et al.* Efficient antigen gene transduction using Arg–Gly–Asp fiber-mutant adenovirus vectors can potentiate antitumor vaccine efficacy and maturation of murine dendritic cells. *Cancer Res* 2001; **61**: 7913–7919.
13 Okada N *et al.* Gene transduction efficiency and maturation status in mouse bone marrow-derived dendritic cells infected with conventional or RGD fiber-mutant adenovirus vectors. *Cancer Gene Ther* 2003; **10**: 421–431.
14 Okada N *et al.* Dendritic cells transduced with gp100 gene by RGD fiber-mutant adenovirus vectors are highly efficacious in generating anti-B16BL6 melanoma immunity in mice. *Gene Therapy* 2003; **10**: 1891–1902.
15 Lanzavecchia A. Identifying strategies for immune intervention. *Science* 1993; **260**: 937–944.
16 Lappin MB *et al.* Analysis of mouse dendritic cell migration *in vivo* upon subcutaneous and intravenous injection. *Immunology* 1999; **98**: 181–188.
17 Martín-Fontecha A *et al.* Regulation of dendritic cell migration to the draining lymph node: impact on T lymphocyte traffic and priming. *J Exp Med* 2003; **198**: 615–621.
18 Kleindienst P, Brocker T. Endogenous dendritic cells are required for amplification of T cell responses induced by dendritic cell vaccines *in vivo*. *J Immunol* 2003; **170**: 2817–2823.
19 Granucci F *et al.* Early events in dendritic cell maturation induced by LPS. *Microbes Infect* 1999; **1**: 1079–1084.
20 Dhodapkar MV *et al.* Antigen-specific inhibition of effector T cell function in human after injection of immature dendritic cells. *J Exp Med* 2001; **193**: 233–238.
21 Steinman RM, Nussenzweig MC. Avoiding horror autotoxicus: the importance of dendritic cells in peripheral T cell tolerance. *Proc Natl Acad Sci USA* 2002; **99**: 351–358.
22 Steinbrink K *et al.* $CD4^+$ and $CD8^+$ anergic T cells induced by interleukin-10-treated human dendritic cells display antigen-specific suppressor activity. *Blood* 2002; **99**: 2468–2476.
23 Mahnke K *et al.* Immature, but not inactive: the tolerogenic function of immature dendritic cells. *Immunol Cell Biol* 2002; **80**: 477–483.
24 Huang FP *et al.* A discrete subpopulation of dendritic cells transports apoptotic intestinal epithelial cells to T cell areas of mesenteric lymph nodes. *J Exp Med* 2000; **191**: 435–444.
25 Hemmi H *et al.* Skin antigens in the steady state are trafficked to regional lymph nodes by transforming growth factor-β1-dependent cells. *Int Immunol* 2001; **13**: 695–704.
26 Yanagawa Y, Onoe K. CCR7 ligands induce rapid endocytosis in mature dendritic cells with concomitant up-regulation of Cdc42 and Rac activities. *Blood* 2003; **101**: 4923–4929.
27 Saeki H, Moore AM, Brown MJ, Hwang ST. Secondary lymphoid-tissue chemokine (SLC) and CC chemokine receptor 7 (CCR7) participate in the emigration pathway of mature dendritic cells from the skin to regional lymph nodes. *J Immunol* 1999; **162**: 2472–2475.
28 Curiel-Lewandrowski C *et al.* Transfection of immature murine bone marrow-derived dendritic cells with the granulocyte-macropharge colony-stimulating factor gene potently enhances their *in vivo* antigen-presenting capacity. *J Immunol* 1999; **163**: 174–183.
29 Hirao M *et al.* CC chemokine receptor-7 on dendritic cell is induced after interaction with apoptotic tumor cells: critical role in migration from the tumor site to draining lymph nodes. *Cancer Res* 2000; **60**: 2209–2217.
30 Wu MT, Hwang ST. CXCR5-transduced bone marrow-derived dendritic cells traffic to B cell zones of lymph nodes and modify antigen-specific immune responses. *J Immunol* 2002; **168**: 5096–5102.
31 Nakamura M *et al.* Dendritic cells genetically engineered to simultaneously express endogenous tumor antigen and

granulocyte macrophage colony-stimulating factor elicit potent therapeutic antitumor immunity. *Clin Cancer Res* 2002; **8**: 2742–2749.

32 de Vries IJM *et al*. Effective migration of antigen-pulsed dendritic cells to lymph nodes in melanoma patients is determined by their maturation state. *Cancer Res* 2003; **63**: 12–17.

33 Eggert AAO *et al*. Analysis of dendritic cell trafficking using EGFP-transgenic mice. *Immunol Lett* 2003; **89**: 17–24.

34 Scandella E *et al*. Prostaglandin E2 is a key factor for CCR7 surface expression and migration of monocyte-derived dendritic cells. *Blood* 2002; **100**: 1354–1361.

35 Scandella E *et al*. CCL19/CCL21-triggered signal transduction and migration of dendritic cells requires prostaglandin E2. *Blood* 2004; **103**: 1595–1601.

36 Sato M *et al*. Generation of mature dendritic cells fully capable of T helper type 1 polarization using OK-432 combined with prostaglandin E_2. *Cancer Sci* 2003; **94**: 1091–1098.

37 Nair S *et al*. Injection of immature dendritic cells into adjuvant-treated skin obviates the need for *ex vivo* maturation. *J Immunol* 2003; **171**: 6275–6282.

38 Pfeifer JD *et al*. Phagocytic processing of bacterial antigens for class I MHC presentation to T cells. *Nature* 1993; **361**: 359–362.

39 Okabe M *et al*. Green mice as a source of ubiquitous green cells. *FEBS Lett* 1997; **407**: 313–319.

40 Mizuguchi H *et al*. A simplified system for constructing recombinant adenoviral vectors containing heterologous peptides in the HI loop of their fiber knob. *Gene Therapy* 2001; **8**: 730–735.

41 Mizuguchi H, Kay MA. Efficient construction of a recombinant adenovirus vector by an improved *in vitro* ligation method. *Hum Gene Ther* 1998; **9**: 2577–2583.

42 Mizuguchi H, Kay MA. A simple method for constructing E1- and E1/E4-deleted recombinant adenoviral vectors. *Hum Gene Ther* 1999; **10**: 2013–2017.

43 Lutz MB *et al*. An advanced culture method for generating large quantities of highly pure dendritic cells from mouse bone marrow. *J Immunol Methods* 1999; **223**: 77–92.

44 Okada N *et al*. Administration route-dependent vaccine efficiency of murine dendritic cells pulsed with antigens. *Br J Cancer* 2001; **84**: 1564–1570.

Available online at www.sciencedirect.com
SCIENCE DIRECT
Biochimica et Biophysica Acta 1670 (2004) 172–180
BIOCHIMICA ET BIOPHYSICA ACTA
BBA
www.bba-direct.com

Optimization of antitumor efficacy and safety of in vivo cytokine gene therapy using RGD fiber-mutant adenovirus vector for preexisting murine melanoma

Yuka Okada[a], Naoki Okada[b,*], Hiroyuki Mizuguchi[c], Koichi Takahashi[a], Takao Hayakawa[d], Tadanori Mayumi[e], Nobuyasu Mizuno[a]

[a] *Department of Pharmaceutics, School of Pharmaceutical Sciences, Mukogawa Women's University, 11-68 Kyuban-cho, Koshien, Nishinomiya, Hyogo 663-8179, Japan*
[b] *Department of Biopharmaceutics, Kyoto Pharmaceutical University, 5 Nakauchi-cho, Misasagi, Yamashina, Kyoto 607-8414, Japan*
[c] *Division of Cellular and Gene Therapy Products, National Institute of Health Sciences, 1-18-1 Kamiyoga, Setagaya, Tokyo 158-8501, Japan*
[d] *National Institute of Health Sciences, 1-18-1 Kamiyoga, Setagaya, Tokyo 158-8501, Japan*
[e] *Department of Biopharmaceutics, Graduate School of Pharmaceutical Sciences, Osaka University, 1-6 Yamadaoka, Suita, Osaka 565-0871, Japan*

Received 16 September 2003; received in revised form 5 December 2003; accepted 5 December 2003

Abstract

We previously reported that RGD fiber-mutant adenovirus vector (AdRGD) was a very useful vector system for in vivo cytokine gene therapy for established murine B16BL6 melanoma. However, intratumoral administration of AdRGD expressing tumor necrosis factor α (AdRGD-TNFα) at high dose revealed not only the dramatic reinforcement of anti-tumor effect but also serious adverse effects, such as body weight reduction and sudden death, caused by high-level TNF-α leakage from the tumor into circulation. These results strongly suggested that the determination of 'limiting dose', which demonstrated therapeutic effectiveness without adverse effect, against each vector was important for the development of appropriate cytokine gene therapy. In the present study, we investigated the efficacy and the safety of AdRGD expressing interleukin-12 (AdRGD-IL12) in murine melanoma model, and determined its limiting dose. Moreover, we demonstrated that combination therapy using AdRGD-IL12 and AdRGD-TNFα at limiting doses or less could achieve more effective tumor regression without adverse effects. Therefore, we conclude that a combination of multiple AdRGD expressing cytokines having distinct anti-tumor mechanisms can contribute to the establishment of in vivo cytokine gene therapy for melanoma, which possesses both excellent efficacy and high safety.

Keywords: Adenovirus vector; Melanoma; Gene therapy; Fiber-mutant; IL-12; TNF-α

1. Introduction

Because the prognosis of patients with melanoma is generally poor and the tumors commonly metastasize [1,2], the development of innovative approaches including gene therapy for treatment of malignant melanoma is imperative for improving the cure rate. To realize the effective gene therapy for melanoma, we have focused on the development of a novel vector system that can improve the gene transduction efficiency against melanoma cells.

We previously demonstrated that RGD fiber-mutant adenovirus vector (AdRGD), which contains an α_v-integrin tropism due to an RGD peptide inserted into the HI loop of the fiber knob, was superior to conventional adenovirus vector (Ad) in gene transduction efficiency to melanoma both in vitro and in vivo [3]. In addition, the intratumoral injection of human tumor necrosis factor α (TNF-α)-expressing AdRGD (AdRGD-TNFα) could more effectively induce hemorrhagic necrosis and regression in established murine B16BL6 melanoma as compared with administration of conventional Ad-TNFα. Although these results suggested that AdRGD was useful for in vivo cytokine gene therapy for melanoma, leakage of TNF-α into systemic circulation from the tumor resulted in serious

Abbreviations: Ad, adenovirus vector; AdRGD, RGD fiber-mutant Ad; CAR, coxsackie-adenovirus receptor; CTL, cytotoxic T lymphocyte; FBS, fetal bovine serum; IFN-γ, interferon γ; IL-12, interleukin 12; NK, natural killer; PBS, phosphate-buffered saline; Th, helper T; TNF-α, tumor necrosis factor α

* Corresponding author. Tel.: +81-75-595-4662; fax: +81-75-595-4761.
E-mail address: okada@mb.kyoto-phu.ac.jp (N. Okada).

0304-4165/$ - see front matter © 2004 Elsevier B.V. All rights reserved.
doi:10.1016/j.bbagen.2003.12.002

adverse effects, including extreme reduction in body weight, in mice that received intratumoral administration of AdRGD-TNFα at high doses [4]. Therefore, further optimization of the in vivo cytokine gene therapy using AdRGD is required to improve efficacy and safety. Our alternative approaches, which can repress the adverse effects by improving the effectiveness per vector dosage, may be the combination of two or more AdRGDs that express distinct cytokines such as TNF-α and interleukin 12 (IL-12).

IL-12 is a 70 kDa (p70) heterodimer protein in which the 40 kDa (p40) and 35 kDa (p35) subunits are connected by one S-S bond [5,6], and plays a key role in the induction of cellular immune responses, such as enhancement of proliferation and cytotoxic activity in natural killer (NK) cells and cytotoxic T lymphocytes (CTL) [7,8], production of interferon-γ (IFN-γ) from activated cells [8–10], and promotion of differentiation of helper T type 1 (Th1) cells from Th0 cells [8,11,12]. IFN-γ is involved in IL-12-mediated tumor regression [13], and IL-12 also exhibits an anti-angiogenic effect that can account for some anti-tumor activity [14]. Because systemic administration of recombinant IL-12 at high doses induces adverse effects associated with high systemic peak concentrations [15,16], the intratumoral administration of a vector carrying the IL-12 gene is a promising approach for efficient induction of antitumor effects and repression of adverse systemic effects due to the persistent local expression of cytokines in the tumor.

In the current study, we investigated the therapeutic efficacy and adverse effects of in vivo gene therapy using IL-12-expressing AdRGD (AdRGD-IL12) in the murine B16BL6 melanoma model and compared the response to that of conventional Ad-IL12. We also attempted to optimize the in vivo cytokine gene therapy protocol for melanoma by combining AdRGD-IL12 and AdRGD-TNFα due to the distinct mechanisms of their antitumor effects.

2. Materials and methods

2.1. Cell lines and mice

Murine melanoma B16BL6 cells were obtained from JCRB cell bank (Tokyo, Japan) and cultured in minimum essential medium supplemented with 5% fetal bovine serum (FBS) and antibiotics. HEK293 cells (JCRB cell bank) were grown in Dulbecco's modified Eagle's medium supplemented with 10% FBS and antibiotics. EL4 cells and YAC-1 cells were purchased from ATCC (Manassas, VA, USA) and cultured in RPMI 1640 medium supplemented with 10% FBS, 50 μM 2-mercaptoethanol, and antibiotics. Female C57BL/6 mice, aged 6–7 weeks, were purchased from SLC Inc. (Hamamatsu, Japan) and held under specified pathogen-free conditions. Animal experimental procedures were in accordance with the Osaka University guidelines for the welfare of animals in experimental neoplasia.

2.2. Vectors

The replication-deficient AdRGD-IL12 and conventional Ad-IL12, which carried the murine IL-12 gene derived from mIL-12 BIA/pBluescript II KS(-) [17] (kindly provided by Dr. Hiroshi Yamamoto; Department of Immunology, Graduate School of Pharmaceutical Sciences, Osaka University, Suita, Japan), were constructed by an improved in vitro ligation method using pAdHM15-RGD and pAdHM4, respectively [18–20]. The expression cassette, which was designed to be transcribed in order from IL-12 p35 cDNA to the internal ribosome entry site sequence to IL-12 p40 cDNA under the control of the cytomegalovirus promoter, was inserted into the E1-deletion region of each E1/E3-deleted Ad vector. The construction of AdRGD-TNFα was described previously [3]. All vectors were propagated in HEK293 cells, purified by two rounds of CsCl gradient centrifugation, dialyzed with phosphate-buffered saline (PBS) containing 10% glycerol, and stored at −80 °C. The number of vector particles (VP) in vector stock was spectrophotometrically determined by the method of Maizel et al. [21].

2.3. Analysis of gene transduction in vitro

B16BL6 cells cultured on 24-well plates were infected with Ad-IL12 or AdRGD-IL12 for 2 h at various VP/cell in 100 μl of FBS-free medium. After washing twice with PBS, a 500-μl aliquot of culture medium was added to each well. Two days later, the supernatants were collected and the IL-12 p70 level was measured using a murine IL-12 p70 ELISA KIT (Biosource International, Camarillo, CA, USA).

2.4. Tumor inoculation and intratumoral administration of vectors in animal experiments

B16BL6 cells were intradermally inoculated into the abdomen of C57BL/6 mice at 2×10^5 cells/mouse. Six days later, established tumors with diameters of 5–7 mm were injected with each vector at various VP in 50-μl PBS.

2.5. In vivo gene transduction analysis

On day 2 after intratumoral Ad-IL12- or AdRGD-IL12-injection at 10^8 or 10^9 VP, B16BL6 tumors were removed, weighed, and homogenized in PBS containing 10 μg/ml aprotinin and 100 μM phenylmethylsulfonyl fluoride. After centrifugation at 15,000 rpm for 30 min, IL-12 p70 levels in the supernatants were measured using ELISA.

2.6. In vivo cytokine gene therapy model

B16BL6 tumor size and body weight in mice intratumorally injected with each vector were measured three times a week, and the tumor volume and the relative body weight were calculated by the following formulas, respectively:

tumor volume (mm^3)=(major axis) × (minor axis)^2 × 0.5236 [22], relative body weight=(body weight after Ad-treatment)/(body weight before Ad-treatment). Mice containing tumors >20 mm were euthanized. On day 90 after tumor challenge, all survivors were euthanized.

2.7. Eu-release assay for cytolytic activity of NK cells and CTLs

Established B16BL6 tumors were injected with Ad-IL12 or AdRGD-IL12 at 10^9 VP. At 1 week after Ad-injection, non-adherent splenocytes were prepared from these mice and directly used as NK effector cells. A surplus of splenocytes was restimulated in vitro using B16BL6 cells, which were cultured in media containing 100 U/ml recombinant murine IFN-γ (PeproTech EC Ltd., London, England) for 24 h and inactivated with 50 μg/ml mitomycin C at 37 °C for 30 min, at an effector/stimulator ratio of 10:1 in RPMI 1640 supplemented with 10% FBS, 50 μM 2-mercaptoethanol, and antibiotics. Five days later, the splenocytes were collected and used as CTL effector cells. Target cells (YAC-1 cells, B16BL6 cells, and EL4 cells) were Eu-labeled and an Eu-release assay was performed as previously described [23]. Cytolytic activity was determined using the following formula: % lysis=[(experimental Eu-release − spontaneous Eu-release)/(maximum Eu-release − spontaneous Eu-release)] × 100. Spontaneous Eu-release of the target cells was < 10% of maximum Eu-release by detergent in all assays.

2.8. In vivo depletion analysis

Mice bearing B16BL6 tumor were intratumorally injected with AdRGD-IL12 at 10^9 VP, and then intraperitoneally injected five times with 100-μl ascites from ICR-nu/nu mice intraperitoneally injected with GK1.5 hybridoma (anti-CD4) [24] or 53-6.72 hybridoma (anti-CD8) [25] (kindly provided by Dr. Hiroshi Yamamoto, Department of Immunology, Graduate School of Pharmaceutical Sciences, Osaka University, Suita, Japan), 40-μl rabbit anti-asialoGM1 antiserum (Wako Chemical, Osaka, Japan), or a mixture of these three antibody reagents at 2-day intervals. Depletion of T cell subsets and NK cells was monitored by flow cytometry, which showed >90% specific depletion in splenocytes at day 4 after the first antibody administration in each protocol.

2.9. Determination of IL-12 and IFN-γ levels in sera from mice intratumorally injected with AdRGD-IL12 or Ad-IL12 at high dose

Blood samples were collected from the tail veins of B16BL6 tumor-bearing mice intratumorally injected with AdRGD-IL12 or Ad-IL12 at 10^{10} or 10^{11} VP. Sera were immediately separated by centrifugation, and combined with 1/9 volume of PBS containing 10 mM EDTA and 100 μg/ml aprotinin. IL-12 and IFN-γ levels in sera were measured using the murine IL-12 p70 ELISA KIT and the murine IFN-γ ELISA KIT (Biosource International), respectively.

3. Results and discussion

Of the existing vector systems for gene therapy, Ad provides the highest transduction efficiency to a wide variety of cell types and tissues, regardless of the mitotic status of the cells [26–29]. Ad can also be easily amplified at high titers and concentrated by centrifugation, thereby facilitating application to gene therapy based on efficient direct in vivo gene delivery for various kinds of diseases [30]. Because of these advantages, Ad is widely used in clinical research of gene therapy as well as retrovirus vector. However, melanoma, which is an important target for gene therapy, requires high Ad dosage for sufficient gene expression. We previously reported that the resistance of melanoma cells to Ad-mediated gene transduction was caused by extremely poor expression of coxsackie-adenovirus receptor (CAR), the primary Ad receptor, on the cell surface, and that AdRGD, which targets α_v-integrins during attachment to cells, exhibited highly efficient foreign gene transduction in melanoma cells as compared with conventional Ad [3]. In the present report, we therefore investigated the efficacy and safety of IL-12 gene therapy using AdRGD on the murine B16BL6 melanoma model, and also tested combination therapy using AdRGD-IL12 and AdRGD-TNFα to optimize in vivo cytokine gene therapy for melanoma.

3.1. Transduction efficiency of IL-12 genes to B16BL6 cells or tumors by AdRGD or conventional Ad

To assess efficiency of productive gene transfer into melanoma cells, we compared the level of IL-12 secretion in supernatants from a 2-day culture of AdRGD-IL12- or Ad-IL12-infected B16BL6 cells (Fig. 1A). The IL-12 levels increased in a VP-dependent manner, and IL-12 secretion from melanoma cells infected with AdRGD-IL12 was about 70-fold and 90-fold higher at 5000 VP/cell and 20,000 VP/cell, respectively, than that from Ad-IL12-infected cells. The viability of B16BL6 cells infected at the highest dose, 20,000 VP/cell, did not change from that of uninfected cells (data not shown), suggesting that IL-12 accumulated in culture media but did not directly injure B16BL6 cells.

Likewise, we compared in vivo gene transduction efficiency of AdRGD-IL12 and Ad-IL12 to B16BL6 tumors established in C57BL/6 mice (Fig. 1B). On day 2 after Ad-treatment, the IL-12 levels in B16BL6 tumors injected with AdRGD-IL12 were 7-fold higher at 10^9 VP/tumor than in Ad-IL12-injected tumors. In addition, AdRGD-IL12 injection at 10^8 VP/tumor attained equal expression of IL-12 in B16BL6 tumors as obtained with Ad-IL12 injection at a 10-fold higher dose, 10^9 VP/tumor. Taken together, these results clearly suggest that AdRGD is a very potent vector

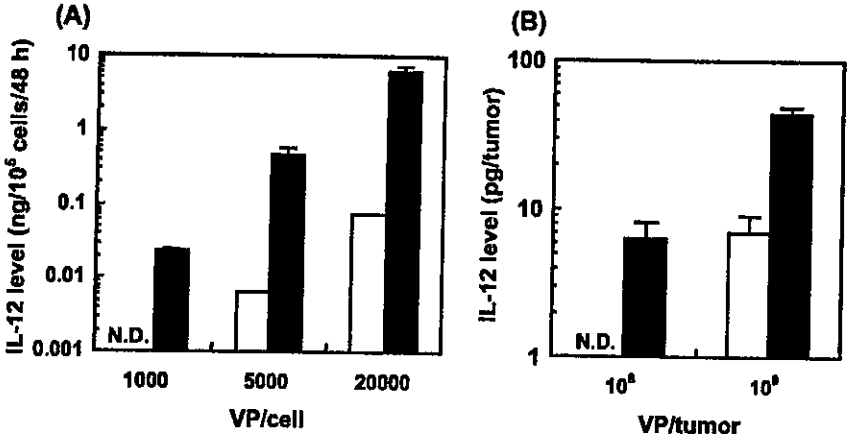

Fig. 1. IL-12 production levels in B16BL6 cells or tumors infected with AdRGD-IL12 or Ad-IL12. (A) B16BL6 cells were infected with Ad-IL12 (open column) or AdRGD-IL12 (closed column) at indicated VP/cell for 2 h. Two days later, the level of IL-12 secreted into culture medium was measured by ELISA. The data represent the mean ± S.D. of three independent cultures. (B) Established B16BL6 tumors with diameters of 5–7 mm in C57BL/6 mice were injected with Ad-IL12 (open column) or AdRGD-IL12 (closed column) at indicated VP/tumor. Two days later, tumors were removed and homogenized in PBS containing 10 μg/ml aprotinin and 100 μM phenylmethylsulfonyl fluoride. The homogenates were centrifuged and the IL-12 level in the supernatants was determined by ELISA. Data are presented as mean ± S.D. of three mice. N.D.: IL-12 level was not detectable.

system for foreign gene transduction in melanoma both in vitro and in vivo, as we showed in our previous studies [3,4,31]. Furthermore, since the majority of tumors is positive for α_v-integrin [32,33] and some tumors exhibit a decline in CAR expression with progressing malignancy [34,35], AdRGD is promising for gene therapy for many advanced cancers as well as melanoma.

3.2. Tumor regression and body weight change in mice intratumorally injected with AdRGD-IL12 or Ad-IL12

We next evaluated the anti-tumor effects following the intratumoral injection of AdRGD-IL12 or Ad-IL12 in the murine B16BL6 melanoma model. As shown in Fig. 2A, tumor growth was inhibited by intratumoral administration of Ad-IL12 or AdRGD-IL12 in a VP-dependent manner, and growth inhibition upon administration of 10^8 AdRGD-IL12 was comparable to that after treatment with 10^9 Ad-IL12. This outcome was positively correlated with IL-12 expression in B16BL6 tumors injected with each Ad type, as shown in Fig. 1B. We therefore determined that AdRGD could reduce the vector dosage in in vivo IL-12 gene therapy to about one-tenth that of conventional Ad while maintaining an equal therapeutic effect against melanoma. The body weight of B16BL6 tumor-bearing mice intratumorally injected with AdRGD-IL12 or Ad-IL12 at a higher dose, 10^{10} or 10^{11} VP/tumor, decreased remarkably for several days after vector administration, although we observed a very strong antitumor effect (Fig. 2B). Based on these results, we determined that the 'limiting dose' of

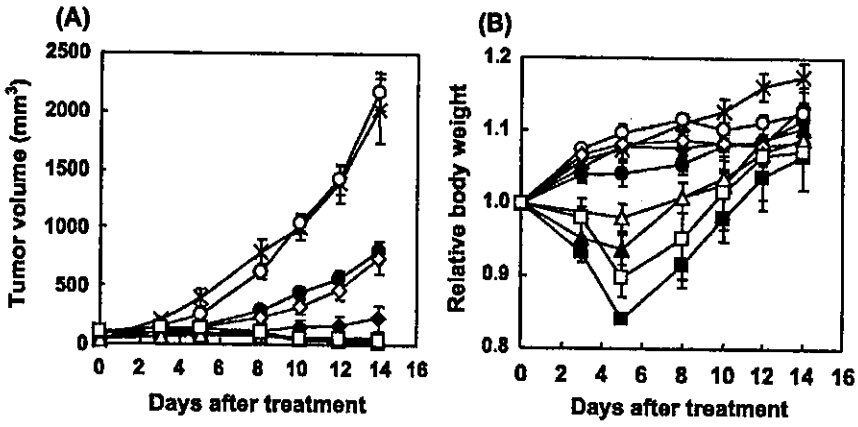

Fig. 2. Anti-B16BL6 tumor effect and body weight change upon an intratumoral administration of Ad-IL12 or AdRGD-IL12. B16BL6 cells were intradermally inoculated into C57BL/6 mice at 2×10^5 cells/mouse. Six days later, the tumors were injected with Ad-IL12 [(○) 10^8, (◇) 10^9, (△) 10^{10}, or (□) 10^{11} VP/tumor], AdRGD-IL12 [(●) 10^8, (◆) 10^9, (▲) 10^{10}, or (■) 10^{11} VP/tumor], or PBS (×). The tumor size and body weight were determined three times a week, and the tumor volume (A) and the relative body weight (B) were calculated according to the formula described in Materials and methods. The data are representative of two independent experiments. Each point represents the mean ± S.E. of four to five mice.

AdRGD-IL12 and Ad-IL12 was 10^9 VP/tumor. This dose provided an anti-tumor effect but did not cause a decrease in body weight.

3.3. Mechanism underlying the improved anti-tumor effects of AdRGD-IL12 application

In order to analyze the mechanism underlying the enhanced anti-B16BL6 tumor effects upon intratumoral injection of AdRGD-IL12, we compared the cytolytic activities of NK cells and B16BL6-specific CTLs in mice injected with AdRGD-IL12 or Ad-IL12 at 10^9 VP/tumor. One week after Ad-treatment, the splenocytes were prepared and directly used in the Eu-release assay for NK-sensitive YAC-1 cells. On the other hand, the surplus of splenocytes was in vitro restimulated for 5 days with inactivated B16BL6 cells, which were pretreated with IFN-γ to promote the expression of their major histocompatibility complex class I molecules, for CTL expansion. As shown in Fig. 3A, the splenic NK activity was augmented after intratumoral injection of AdRGD-IL12 or Ad-IL12 as compared with tumor-free (intact) mice or B16BL6 tumor-bearing mice intratumorally injected with PBS, and the highest cytolytic activity was detected in the AdRGD-IL12-injected group. In vitro restimulated effector cells from the PBS-injected group revealed lower cytolytic activity than those from intact mice (Fig. 3B). This phenomenon suggested that differentiation, antigen priming, and/or activation of T cells might be suppressed in B16BL6 tumor-bearing mice. Nevertheless, intratumoral injection of Ad-IL12 could increase cytolytic activity of CTL effector against B16BL6 cells, and more potent activity was detected in restimulated splenocytes from AdRGD-IL12-injected mice. Because no cytolytic effects against syngeneic irrelevant EL4 cells were detected in restimulated effector cells from any group (Fig. 3C), it was confirmed that cytolytic activities in Fig. 3B were caused by B16BL6-specific CTLs. Therefore, the enhancement of both nonspecific NK activity and B16BL6-specific CTL activity might improve the anti-B16BL6 melanoma response to intratumoral injection of AdRGD-IL12.

Furthermore, in order to confirm that NK cells and CTLs were the major effector cells responsible for B16BL6 tumor regression in mice intratumorally injected with AdRGD-IL12, we performed in vivo depletion analysis using specific antibodies against CD4, CD8, and asialoGM1 (Fig. 4). The depletion of $CD8^+$ T cells or NK cells weakened the anti-tumor efficacy induced by intratumoral injection of AdRGD-IL12, whereas tumor growth inhibition was not affected by $CD4^+$ T cell depletion. Additionally, the anti-tumor effect was more notably suppressed by depletion of three kinds of lymphocyte subsets. These results clearly demonstrated that $CD8^+$ CTLs and NK cells were the predominant effector cells in anti-B16BL6 melanoma immunity induced by intratumoral injection of AdRGD-IL12.

3.4. Adverse effects in mice intratumorally injected with AdRGD-IL12 or Ad-IL12 at high dose

Gene therapy that induces locally persistent cytokine production is an attractive strategy for preventing severe adverse effects upon systemic administration of cytokines at high dose. Cytokine gene therapy represents about 20% of

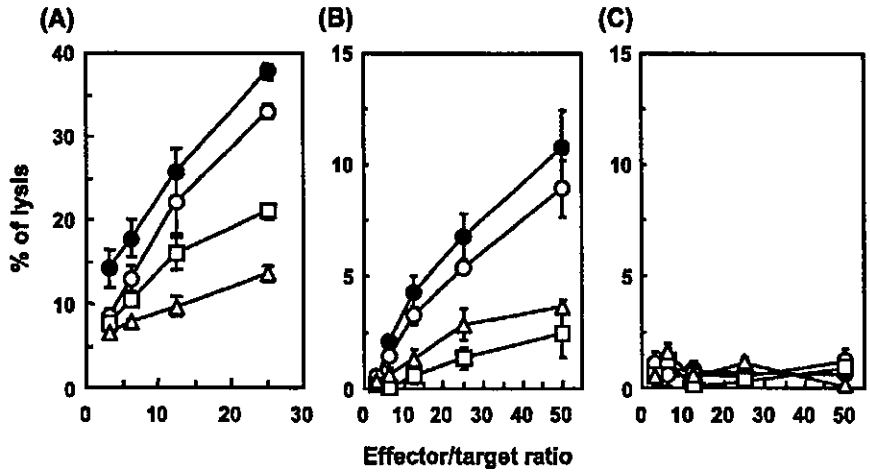

Fig. 3. NK activity and B16BL6-specific CTL activity of splenocytes from mice injected intratumorally with AdRGD-IL12 or Ad-IL12. B16BL6 cells were intradermally inoculated into C57BL/6 mice at 2×10^5 cells/mouse. Six days later, the tumors were injected with Ad-IL12 at 10^9 VP/tumor (○), AdRGD-IL12 at 10^9 VP/tumor (●), or PBS (□). At 1 week after treatment, non-adherent splenocytes were prepared from these mice. Likewise, splenocytes from tumor-free (intact) mice (△) were prepared. Splenocytes were directly used in cytolytic assays against NK-sensitive YAC-1 cells (A), or restimulated in vitro for 5 days with IFN-γ-stimulated and mitomycin C-inactivated B16BL6 cells for CTL expansion. A cytolytic assay for CTL effector was performed using B16BL6 cells (B) and syngeneic irrelevant EL4 cells (C). Cytolytic activity (% lysis) was calculated according to the formula described in Materials and methods. Each point represents the mean ± S.E. from three independent cultures using splenocytes prepared from three individual mice.

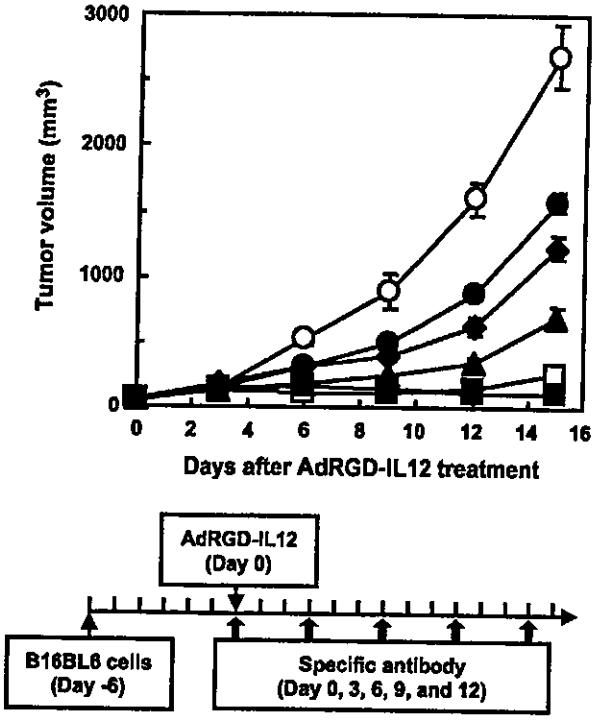

Fig. 4. Determination of immune subsets responsible for B16BL6 tumor regression induced by intratumoral administration of AdRGD-IL12. B16BL6 cells were intradermally inoculated into C57BL/6 mice at 2×10^5 cells/mouse. Six days later, the tumors were injected with AdRGD-IL12 at 10^9 VP/tumor (□), or PBS (○). The antibodies GK1.5 (anti-CD4) alone (■), 53-6.72 (anti-CD8) alone (▲), anti-asialoGM1 alone (♦), or combination of these three antibodies (●), were intraperitoneally injected according to the indicated schedule. Depletion of T cell subsets and NK cells was monitored by flow cytometry, which showed >90% specific depletion in splenocytes at day 4 after the first antibody administration. Each point represents the mean ± S.E. of six mice.

total clinical research protocols for gene therapy. However, we observed an extreme reduction in body weight in addition to tumor regression in mice intratumorally injected with AdRGD-IL12 or Ad-IL12 at high dose (Fig. 2). This result agrees with our previous study using AdRGD-TNFα and suggests that IL-12, which is expected to leak from the tumors into circulation, may be a cause of the adverse effects [4]. Because identification of the mechanism causing adverse effects is important for establishing the clinical protocol for in vivo cytokine gene therapy, we investigate the correlation between serum IL-12 concentrations and body weight change in mice injected intratumorally with Ad-IL12 or AdRGD-IL12 at 10^{10} or 10^{11} VP (Fig. 5A and C). Mice injected with AdRGD-IL12 or Ad-IL12 at 10^{11} VP/tumor exhibited 6–10 ng IL-12/ml serum on day 1 after Ad-treatment, which then rapidly decreased. Although the maximum body weight reduction in these mice was observed on days 5–6 after Ad-treatment, serum IL-12 concentration was 0.2 ng/ml at this time. Therefore, the rise in IL-12 concentration in the blood was not the direct cause of body weight reduction in mice treated with IL-12-expressing vector at high dose. Because the antitumor properties of IL-12 are mediated in large part by IFN-γ, we simultaneously measured IFN-γ concentrations in sera from these mice. Despite the 20-min half-life of IFN-γ in blood, serum IFN-γ levels were dramatically elevated up to 5 days after Ad-treatment in mice treated with 10^{11} VP of each vector, and the IFN-γ profile in sera was well correlated with body weight changes in all tested groups (Fig. 5B). Serum IL-12 and IFN-γ concentrations were undetectable in mice intravenously injected with 10^{10} AdRGD-IL12 or intratumorally injected with 10^9 AdRGD-IL12 or 10^{11} AdRGD-Luc, which was the control vector expressing firefly luciferase (data not shown), and weight reduction was not observed. Additionally, TNF-α, which is known to be secreted from responder cells by IL-12 stimulation, was only detected at low levels (0.1–0.2 ng/ml) in sera from mice treated with 10^{11} VP of each vector on days 5 and 7 after Ad-treatment (data not shown). These results strongly suggested that the adverse effects observed in mice injected intratumorally with Ad-IL12 or AdRGD-IL12 at high dose were caused by a systemic inflammatory reaction triggered by high levels of endogenous IFN-γ. The secondary production of endogenous IFN-γ was induced by the leakage of IL-12 from Ad-treated B16BL6 tumors. Therefore, to ensure the safety of in vivo cytokine gene therapy using AdRGD for melanoma, we must avoid protocols that include high-levels of cytokines, which leak into the circulating blood from the tumor.

3.5. Combination therapy using AdRGD-IL12 and AdRGD-TNFα for B16BL6 melanoma

In our experimental model, the limiting dose of AdRGD-IL12 that demonstrated effective tumor regression without a rise in serum cytokine levels was 10^9 VP/tumor. We previously found that the limiting dose of AdRGD-TNFα was also 10^9 VP/tumor in a similar experiment [4]. Identification of a limiting dose is important for continued progress in research and development of the in vivo cytokine gene therapy. In order to further improve efficacy while remaining below the limiting dose, we must evaluate combination therapy using two or more vectors that express distinct cytokines and possess varying therapeutic mechanisms, rather than relying on the therapeutic effects of a single cytokine-expressing vector. Additionally, several reports demonstrated a concept to reinforce the anti-tumor efficacy in murine melanoma model by combination of IL-12 and TNF-α [36,37]. Therefore, we evaluated the effects of intratumoral co-injection of AdRGD-IL-12 and AdRGD-TNFα at the limiting dose or below. B16BL6 tumors injected with a mixture of 5×10^8 AdRGD-IL12 and 5×10^8 AdRGD-TNFα demonstrated more effective regression than tumors injected with either AdRGD-IL12 or AdRGD-TNFα alone at 10^9 VP (Fig. 6A). Furthermore, all six mice co-injected with 10^9 AdRGD-IL12 and 10^9 AdRGD-TNFα achieved complete regression of established B16BL6 tumors and remained tumor-free until day 90 after tumor challenge. On the other hand, no reduction

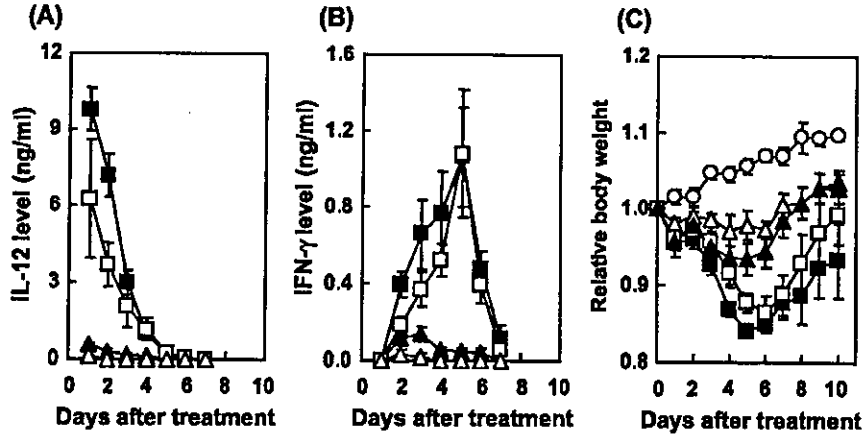

Fig. 5. IL-12 level (A) or IFN-γ level (B) in sera, and body weight change (C) upon intratumoral administration of Ad-IL12 or AdRGD-IL12 at 10^{10} or 10^{11} VP. B16BL6 cells were intradermally inoculated into C57BL/6 mice at 2×10^5 cells/mouse. The tumors (5–7 mm in diameter) were injected with Ad-IL12 [(△) 10^{10}, or (□) 10^{11} VP/tumor], AdRGD-IL12 [(▲) 10^{10}, or (■) 10^{11} VP/tumor], or PBS (○). IL-12 (A) and IFN-γ (B) concentrations in sera from these mice were measured using the murine IL-12 ELISA kit and murine IFN-γ ELISA kit, respectively. Relative body weight (C) was calculated according to the formula described in Materials and methods. The data are representative of two independent experiments. Each point represents the mean ± S.E. of five mice.

in body weight was observed in any group (Fig. 6B) and serum concentrations of IL-12 and TNF-α were less than the detection limit in mice co-injected with two vectors (data not shown). These results strongly suggest that intratumoral co-injection of multiple cytokine-expressing AdRGDs is a promising strategy capable of improving therapeutic efficacy and suppressing adverse effects of in vivo cytokine gene therapy for melanoma. In addition, other groups have also reported that the application of multiple cytokine genes could demonstrate synergistic therapeutic effects even if gene therapy using a single cytokine gene was ineffective [38–40].

In conclusion, in order to optimize in vivo cytokine gene therapy, we must examine the effectiveness and safety of single cytokine-expressing vectors and of multiple vector combinations, which can be selected based on the mechanisms of efficacy and extent of adverse effects.

Acknowledgements

We are grateful to Dr. Hiroshi Yamamoto (Department of Immunology, Graduate School of Pharmaceutical Sciences, Osaka University) for providing mIL-12 BIA/pBluescript II KS(−), GK1.5 ascites, and 53-6.72 ascites; to Yasushige Masunaga (Department of Biopharmaceutics, Kyoto Pharmaceutical University) for technical assistance with the Eu-release assay; and to Kae Suzuki and Saki Tanaka (Department of Pharmaceutics, School of Pharmaceutical

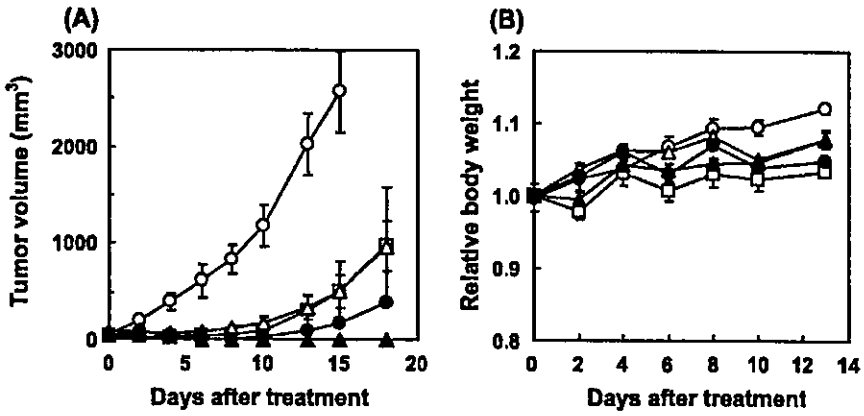

Fig. 6. Anti-B16BL6 tumor effect and body weight change in response to a combination of AdRGD-IL12 and AdRGD-TNFα. B16BL6 cells were intradermally inoculated into C57BL/6 mice at 2×10^5 cells/mouse. Six days later, the tumors were injected with 10^9 AdRGD-IL12 alone (△), 10^9 AdRGD-TNFα alone (□), a combination of 5×10^8 AdRGD-IL12 and 5×10^8 AdRGD-TNFα (●), a combination of 10^9 AdRGD-IL12 and 10^9 AdRGD-TNFα (▲), or PBS (○). The tumor volume (A) and the relative body weight (B) were calculated according to the formula described in Materials and methods. The data are representative of two independent experiments. Each point represents the mean ± S.E. of three to six mice.

Sciences, Mukogawa Women's University) for assistance with animal experiments.

This study was supported in part by grants from the Ministry of Health and Welfare in Japan.

References

[1] A. Schneeberger, M. Goos, G. Stingl, S.N. Wagner, Management of malignant melanoma: new developments in immune and gene therapy, Clin. Exp. Dermatol. 25 (2000) 509–519.

[2] J.K. Wildemore IV, L. Schuchter, R. Mick, M. Synnestvedt, R. Elenitsas, I. Bedrosian, B.J. Czerniecki, D. Guerry IV, S.R. Lessin, D.E. Elder, L.P. Bucky, Locally recurrent malignant melanoma characteristics and outcomes: a single-institution study, Ann. Plast. Surg. 46 (2001) 488–494.

[3] Y. Okada, N. Okada, S. Nakagawa, H. Mizuguchi, K. Takahashi, N. Mizuno, T. Fujita, A. Yamamoto, T. Hayakawa, T. Mayumi, Tumor necrosis factor α-gene therapy for an established murine melanoma using RGD (Arg-Gly-Asp) fiber-mutant adenovirus vectors, Jpn. J. Cancer Res. 93 (2002) 436–444.

[4] Y. Okada, N. Okada, H. Mizuguchi, T. Hayakawa, T. Mayumi, N. Mizuno, An investigation of adverse effects caused by the injection of high-dose TNFα-expressing adenovirus vector into established murine melanoma, Gene Ther. 10 (2003) 700–705.

[5] U. Gubler, A.O. Chua, D.S. Schoenhaut, C.M. Dwyer, W. McComas, R. Motyka, N. Nabavi, A.G. Wolitzky, P.M. Quinn, P.C. Familletti, M.K. Gately, Coexpression of two distinct genes is required to generate secreted bioactive cytotoxic lymphocyte maturation factor, Proc. Natl. Acad. Sci. U. S. A. 88 (1991) 4143–4147.

[6] S.F. Wolf, P.A. Temple, M. Kobayashi, D. Young, M. Dicig, L. Lowe, R. Dzialo, L. Fitz, C. Ferenz, R.M. Hewick, K. Kelleher, S.T. Herrmann, S.C. Clark, L. Azzoni, S.H. Chan, G. Trinchieri, B. Perussia, Cloning of cDNA for natural killer cell stimulatory factor, a heterodimeric cytokine with multiple biologic effects on T and natural killer cells, J. Immunol. 146 (1991) 3074–3081.

[7] M.J. Robertson, R.J. Soiffer, S.F. Wolf, T.J. Manley, C. Donahue, D. Young, S.H. Herrmann, J. Ritz, Response of human natural killer (NK) cells to NK cell stimulatory factor (NKSF): cytolytic activity and proliferation of NK cells are differentially regulated by NKSF, J. Exp. Med. 175 (1992) 779–788.

[8] M.J. Brunda, Interleukin-12, J. Leukoc. Biol. 55 (1994) 280–288.

[9] S.H. Chan, B. Perussia, J.W. Gupta, M. Kobayashi, M. Pospisil, H.A. Young, S.F. Wolf, D. Young, S.C. Clark, G. Trinchieri, Induction of interferon-γ production by natural killer cell stimulatory factor: characterization of the responder cells and synergy with other inducers, J. Exp. Med. 173 (1991) 869–879.

[10] S.H. Chan, M. Kobayashi, D. Santoli, B. Perussia, G. Rinchieri, Mechanisms of IFN-γ induction by natural killer cell stimulatory factor (NKSF/IL-12). Role of transcription and mRNA stability in the synergistic interaction between NKSF and IL-2, J. Immunol. 148 (1992) 92–98.

[11] C.S. Hsieh, S.E. Macatonia, C.S. Tripp, S.F. Wolf, A. O'Garra, K.M. Murphy, Development of TH1 $CD4^+$ T cells through IL-12 produced by Listeria-induced macrophages, Science 260 (1993) 547–549.

[12] R.A. Seder, R. Gazzinelli, A. Sher, W.E. Paul, Interleukin 12 acts directly on $CD4^+$ T cells to enhance priming for interferon γ production and diminishes interleukin 4 inhibition of such priming, Proc. Natl. Acad. Sci. U. S. A. 90 (1993) 10188–10192.

[13] C.L. Nastala, H.D. Edington, T.G. McKinney, H. Tahara, M.A. Nalesnik, M.J. Brunda, M.K. Gately, S.F. Wolf, R.D. Schreiber, W.J. Storkus, Recombinant IL-12 administration induces tumor regression in association with IFN-γ production, J. Immunol. 153 (1994) 1697–1706.

[14] E.E. Voest, B.M. Kenyon, M.S. O'Reilly, G. Truitt, R.J. D'Amato, J. Folkman, Inhibition of angiogenesis in vivo by interleukin 12, J. Natl. Cancer Inst. 87 (1995) 581–586.

[15] J.P. Leonard, M.L. Sherman, G.L. Fisher, L.J. Buchanan, G. Larsen, M.B. Atkins, J.A. Sosman, J.P. Dutcher, N.J. Vogelzang, J.L. Ryan, Effects of single-dose interleukin-12 exposure on interleukin-12-associated toxicity and interferon-γ production, Blood 90 (1997) 2541–2548.

[16] M.B. Atkins, M.J. Robertson, M. Gordon, M.T. Lotze, M. DeCoste, J.S. DuBois, J. Ritz, A.B. Sandler, H.D. Edington, P.D. Garzone, J.W. Mier, C.M. Canning, L. Battiato, H. Tahara, M.L. Sherman, Phase I evaluation of intravenous recombinant human interleukin 12 in patients with advanced malignancies, Clin. Cancer Res. 3 (1997) 409–417.

[17] S. Obana, H. Miyazawa, E. Hara, T. Tamura, H. Nariuchi, M. Takata, S. Fujimoto, H. Yamamoto, Induction of anti-tumor immunity by mouse tumor cells transfected with mouse interleukin-12 gene, Jpn. J. Med. Sci. Biol. 48 (1995) 221–236.

[18] H. Mizuguchi, M.A. Kay, Efficient construction of a recombinant adenovirus vector by an improved in vitro ligation method, Hum. Gene Ther. 9 (1998) 2577–2583.

[19] H. Mizuguchi, M.A. Kay, A simple method for constructing E1- and E1/E4-deleted recombinant adenoviral vectors, Hum. Gene Ther. 10 (1999) 2013–2017.

[20] H. Mizuguchi, N. Koizumi, T. Hosono, N. Utoguchi, Y. Watanabe, M.A. Kay, T. Hayakawa, A simplified system for constructing recombinant adenoviral vectors containing heterologous peptides in the HI loop of their fiber knob, Gene Ther. 8 (2001) 730–735.

[21] J.V. Maizel Jr., D.O. White, M.D. Scharff, The polypeptides of adenovirus. I. Evidence for multiple protein components in the virion and a comparison of types 2, 7A, and 12, Virology 36 (1968) 115–125.

[22] P. Janik, P. Briand, N.R. Hartmann, The effect of estrone-progesterone treatment on cell proliferation kinetics of hormone-dependent GR mouse mammary tumours, Cancer Res. 35 (1975) 3698–3704.

[23] N. Okada, M. Tsujino, Y. Hagiwara, A. Tada, Y. Tamura, K. Mori, T. Saito, S. Nakagawa, T. Mayumi, T. Fujita, A. Yamamoto, Administration route-dependent vaccine efficiency of murine dendritic cells pulsed with antigens, Br. J. Cancer 84 (2001) 1564–1570.

[24] D.P. Dialynas, Z.S. Quan, K.A. Wall, A. Pierres, J. Quintans, M.R. Loken, M. Pierres, F.W. Fitch, Characterization of the murine T cell surface molecule, designated L3T4, identified by monoclonal antibody GK1.5: similarity of L3T4 to the human Leu-3/T4 molecule, J. Immunol. 131 (1983) 2445–2451.

[25] J.A. Ledbetter, L.A. Herzenberg, Xenogeneic monoclonal antibodies to mouse lymphoid differentiation antigens, Immunol. Rev. 47 (1979) 63–90.

[26] M.A. Kay, S.L. Woo, Gene therapy for metabolic disorders, Trends Genet. 10 (1994) 253–257.

[27] K.F. Kozarsky, J.M. Wilson, Gene therapy: adenovirus vectors, Curr. Opin. Genet. Dev. 3 (1993) 499–503.

[28] B. Breyer, W. Jiang, H. Cheng, L. Zhou, R. Paul, T. Feng, T.C. He, Adenoviral vector-mediated gene transfer for human gene therapy, Curr. Gene Ther. 1 (2001) 149–162.

[29] S.A. Vorburger, K.K. Hunt, Adenoviral gene therapy, Oncologist 7 (2002) 46–59.

[30] K. Benihoud, P. Yeh, M. Perricaudet, Adenovirus vectors for gene delivery, Curr. Opin. Biotechnol. 10 (1999) 440–447.

[31] Y. Okada, N. Okada, S. Nakagawa, H. Mizuguchi, M. Kanehira, N. Nishino, K. Takahashi, N. Mizuno, T. Hayakawa, T. Mayumi, Fiber-mutant technique can augment gene transduction efficacy and anti-tumor effects against established murine melanoma by cytokine-gene therapy using adenovirus vectors, Cancer Lett. 177 (2002) 57–63.

[32] N. Chattopadhyay, A. Chatterjee, Studies on the expression of αvβ3 integrin receptors in non-malignant and malignant human cervical tumor tissues, J. Exp. Clin. Cancer Res. 20 (2001) 269–275.

[33] M.D. Sachs, K.A. Rauen, M. Ramamurthy, J.L. Dodson, A.M. De Marzo, M.J. Putzi, M.P. Schoenberg, R. Rodriguez, Integrin αv

and coxsackie adenovirus receptor expression in clinical bladder cancer, Urology 60 (2002) 531–536.
[34] K.A. Rauen, D. Sudilovsky, J.L. Le, K.L. Chew, B. Hann, V. Schmitt, L.D. Schmitt, F. McCormick, Expression of the coxsackie adenovirus receptor in normal prostate and in primary and metastatic prostate carcinoma: potential relevance to gene therapy, Cancer Res. 62 (2002) 3812–3818.
[35] Y.S. Haviv, J.L. Blackwell, A. Kanerva, P. Nagi, V. Krasnykh, I. Dmitriev, M. Wang, S. Naito, X. Lei, A. Hemminki, D. Carey, D.T. Curiel, Adenoviral gene therapy for renal cancer requires retargeting to alternative cellular receptors, Cancer Res. 62 (2002) 4273–4281.
[36] W. Lasek, W. Feleszko, J. Gołąb, T. Stokłosa, M. Marczak, A. Dąbrowska, M. Malejczyk, M. Jakóbisiak, Antitumor effects of the combination immunotherapy with interleukin-12 and tumor necrosis factor α in mice, Cancer Immunol. Immunother. 45 (1997) 100–108.
[37] W. Lasek, A. Mackiewicz, A. Czajka, T. Świtaj, J. Gołąb, M. Wiznerowicz, G. Korczak-Kowalska, E.Z. Bakowiec-Iskra, K. Gryska, D. Iżycki, M. Jakóbisiak, Antitumor effects of the combination therapy with TNF-α gene-modified tumor cells and interleukin 12 in a melanoma model in mice, Cancer Gene Ther. 7 (2000) 1581–1590.
[38] C.L. Addison, J.L. Bramson, M.M. Hitt, W.J. Muller, J. Gauldie, F.L. Graham, Intratumoral coinjection of adenoviral vectors expressing IL-2 and IL-12 results in enhanced frequency of regression of injected and untreated distal tumors, Gene Ther. 5 (1998) 1400–1409.
[39] P.C. Emtage, Y. Wan, M. Hitt, F.L. Graham, W.J. Muller, A. Zlotnik, J. Gauldie, Adenoviral vectors expressing lymphotactin and interleukin 2 or lymphotactin and interleukin 12 synergize to facilitate tumor regression in murine breast cancer models, Hum. Gene Ther. 10 (1999) 697–709.
[40] Y. Liu, H. Huang, A. Saxena, J. Xiang, Intratumoral coinjection of two adenoviral vectors expressing functional interleukin-18 and inducible protein-10, respectively, synergizes to facilitate regression of established tumors, Cancer Gene Ther. 9 (2002) 533–542.

Available online at www.sciencedirect.com
SCIENCE DIRECT®
Biochemical and Biophysical Research Communications 317 (2004) 68–76
BBRC
www.elsevier.com/locate/ybbrc

Anti-tumor activity of chemokine is affected by both kinds of tumors and the activation state of the host's immune system: implications for chemokine-based cancer immunotherapy☆

Naoki Okada,[a,*] Jian-Qing Gao,[b,c,*] Akinori Sasaki,[a] Masakazu Niwa,[a] Yuka Okada,[d] Takashi Nakayama,[e] Osamu Yoshie,[e] Hiroyuki Mizuguchi,[f] Takao Hayakawa,[g] Takuya Fujita,[a] Akira Yamamoto,[a] Yasuo Tsutsumi,[b] Tadanori Mayumi,[b] and Shinsaku Nakagawa[b,*]

[a] *Department of Biopharmaceutics, Kyoto Pharmaceutical University, 5 Nakauchi-cho, Misasagi, Yamashina-ku, Kyoto 607-8414, Japan*
[b] *Department of Biopharmaceutics, Graduate School of Pharmaceutical Sciences, Osaka University, 1-6 Yamadaoka, Suita, Osaka 565-0871, Japan*
[c] *Department of Pharmaceutics, School of Pharmaceutical Sciences, Zhejiang University, 353 Yanan Road, Hangzhou, Zhejiang 310031, PR China*
[d] *Department of Pharmaceutics, School of Pharmaceutical Sciences, Mukogawa Women's University, 11-68 Kyuban-cho, Koshien, Nishinomiya, Hyogo 663-8179, Japan*
[e] *Department of Microbiology, Kinki University School of Medicine, Osaka-Sayama, Osaka 589-8511, Japan*
[f] *Division of Cellular and Gene Therapy Products, National Institute of Health Sciences, 1-18-1 Kamiyoga, Setagaya-ku, Tokyo 158-8501, Japan*
[g] *National Institute of Health Sciences, 1-18-1 Kamiyoga, Setagaya-ku, Tokyo 158-8501, Japan*

Received 23 February 2004

Abstract

In this study, we screened the anti-tumor activity of murine chemokines including CCL17, CCL19, CCL20, CCL21, CCL22, CCL27, XCL1, and CX3CL1 by inoculating murine B16BL6, CT26, or OV-HM tumor cells, all of which were transfected with chemokine-expressing fiber-mutant adenovirus vector, into immunocompetent mice. A tumor-suppressive effect was observed in mice inoculated with CCL19/B16BL6 and XCL1/B16BL6, and CCL22/OV-HM showed considerable retardation in tumor growth. In the cured mice inoculated with CCL22/OV-HM, a long-term specific immune protection against parental tumor was developed. However, we were unable to identify the chemokine that had a suppressive activity common to all three tumor models. Furthermore, an experiment using chemokine-transfected B16BL6 cells was also performed on mice sensitized with melanoma-associated antigen. A drastic enhancement of the frequency of complete rejection was observed in mice inoculated with CCL17-, CCL19-, CCL22-, and CCL27-transfected B16BL6. Altogether, our results suggest that the tumor-suppressive activity of chemokine-gene immunotherapy is greatly influenced by the kind of tumor and the activation state of the host's immune system.

Keywords: Adenovirus vector; Chemokine; Transfection; Anti-tumor activity; Gene immunotherapy

Chemokine consists of a superfamily of small (8–14 kDa), secreted basic proteins that regulate relevant leukocyte-migration and -invasion into tissue by interacting with their specific receptors, which belong to the superfamily of seven-transmembrane domain G-protein-coupled receptors [1,2]. The function of chemokine, which is capable of attracting specific immune cells, is demonstrated in inflammatory disease sites as well as normal lymphoid tissues [2]. Because of these properties, chemokine is considered as the intriguing molecule for cancer immunotherapy, which is based on the premise of

☆ *Abbreviations:* Ad, adenovirus vector; AdRGD, RGD fiber-mutant Ad; CTL, cytotoxic T lymphocyte; DC, dendritic cell; FBS, fetal bovine serum; MOI, multiplicity of infection; NK, natural killer; PBS, phosphate-buffered saline; $TCID_{50}$, tissue culture infectious $dose_{50}$.

* Corresponding authors. Fax: +81-75-595-4761 (N. Okada), +81-6-6879-8179 (S. Nakagawa), +86-571-87217376 (J.-Q. Gao).
E-mail addresses: okada@mb.kyoto-phu.ac.jp (N. Okada), gaojq@phs.osaka-u.ac.jp (J.-Q. Gao), nakagawa@phs.osaka-u.ac.jp (S. Nakagawa).

0006-291X/$ - see front matter © 2004 Elsevier Inc. All rights reserved.
doi:10.1016/j.bbrc.2004.03.013

the eradication of tumor cells as a consequence of interaction with immune cells that have migrated and accumulated in tumor tissues [3]. To date, more than 40 chemokines have been identified, and several chemokines have been demonstrated as candidates for cancer treatment for use either as sole agents or with an adjuvant [4–8].

We hypothesized that efficient in vitro transfection of chemokine gene into tumor cells could render the tumor sufficient chemokine expression in vivo for screening anti-tumor activity. The chemokine, secreted from inoculated tumor cells, would induce the accumulation of immune cells in the tumor tissue. Consequently, the interaction between the immune cells and the tumor cells should initiate and/or demonstrate the anti-tumor immune response. Among the various methods of gene transduction, recombinant adenovirus vector (Ad) can provide high-level transduction efficacy to a variety of cell types [9,10]. However, some tumor cells exhibit a resistance to Ad-mediated gene transduction due to a decline in the expression of a coxsackie-adenovirus receptor, a primary Ad-receptor, on their surface. We previously demonstrated that, compared with conventional Ad, the fiber-mutant Ad harboring the RGD sequence in the HI loop of the fiber knob (AdRGD) could more efficiently transduce foreign genes into several kinds of tumor cells due to their directivity to αv-integrin positive in the majority of tumors [11–13]. Therefore, chemokine-expressing AdRGD would be useful not only for screening the anti-tumor activity of chemokines by in vitro transfection, but also for developing in vivo cancer gene immunotherapy.

In the present study, we first confirmed the vector performance of eight AdRGDs encoding each mouse chemokine, CCL17, CCL19, CCL20, CCL21, CCL22, CCL27, XCL1, or CX3CL1. The anti-tumor activity of these chemokines was investigated in mice by inoculating three kinds of murine tumor cells, B16BL6 melanoma, CT26 colon carcinoma, and OV-HM ovarian carcinoma cells, transfected with each chemokine-expressing AdRGD. In addition, we examined the growth and rejection ratio of chemokine gene-transduced B16BL6 cells in mice sensitized with melanoma-associated antigen (gp100).

Materials and methods

Cell lines and animals. Human lung carcinoma A549 cells were purchased from ATCC (Manassas, VA, USA). Murine melanoma B16BL6 cells (H-2^b) and human embryonic kidney 293 cells were obtained from JCRB cell bank (Tokyo, Japan). Murine colon carcinoma CT26 cells (H-2^d) were kindly provided by Dr. Nicholas P. Restifo (National Cancer Institute, Bethesda, MD, USA). Murine ovarian carcinoma OV-HM cells (H-$2^{b/k}$) were kindly provided by Dr. Hiromi Fujiwara (School of Medicine, Osaka University, Osaka, Japan). A549 and 293 cells were maintained in Dulbecco's modified Eagle's medium supplemented with 10% fetal bovine serum (FBS) and antibiotics. B16BL6 cells were cultured in a minimum essential medium supplemented with 7.5% FBS and antibiotics. CT26 and OV-HM cells were grown in an RPMI 1640 medium supplemented with 10% FBS and antibiotics. Murine pre-B lymphoma L1.2 cells and their stable transfectants of a specific chemokine receptor, L1.2/CCR4, L1.2/CCR6, L1.2/CCR7, L1.2/CCR10, L1.2/XCR1, and L1.2/CX3CR1 cells [14], were maintained in an RPMI 1640 medium supplemented with 10% FBS, 50 μM of 2-mercaptoethanol, and antibiotics. All the cell lines were cultured at 37 °C in a humidified atmosphere with 5% CO_2. Female C57BL/6 (H-2^b), BALB/c (H-2^d), and B6C3F1 (H-$2^{b/k}$) mice, ages 7–8 weeks, were purchased from SLC (Hamamatsu, Japan). All of the animal experimental procedures were in accordance with the Osaka University guidelines for the welfare of animals in experimental neoplasia.

Vectors. Replication-deficient AdRGD was based on the adenovirus serotype 5 backbone with deletions of E1/E3 region. The RGD sequence for αv-integrin-targeting was inserted into the HI loop of the fiber knob using a two-step method as previously described [11]. Mouse cDNAs of CCL17, CCL19, CCL20, CCL21, CCL22, and XCL1 were obtained from pExCell-mCCL17, pT7T3D-Pac-mCCL19, pFastBac1-mCCL20, pT7T3D-Pac-mCCL21, pBluescript SK(+)-mCCL22, and pExCell-mXCL1, respectively. The expression cassette containing each mouse chemokine cDNA under the control of the cytomegalovirus promoter was inserted into E1-deletion site for constructing AdRGD-CCL17, -CCL19, -CCL20, -CCL21, -CCL22, and -XCL1, respectively, by an improved in vitro ligation method as previously described [15,16]. Mouse CCL27-expressing AdRGD (AdRGD-CCL27), mouse CX3CL1-expressing AdRGD (AdRGD-CX3CL1), gp100-expressing AdRGD (AdRGD-gp100), β-galactosidase-expressing AdRGD (AdRGD-LacZ), luciferase-expressing AdRGD (AdRGD-Luc), and AdRGD-Null, which is identical to the AdRGD vectors without the gene expression cassette, were previously constructed [11,17–19]. AdRGD-LacZ, -Luc, and -Null were used as negative control vectors in the present study. All recombinant AdRGDs were propagated in 293 cells, purified by two rounds of cesium chloride gradient ultracentrifugation, dialyzed, and stored at −80 °C. Titers (tissue culture infectious $dose_{50}$; $TCID_{50}$) of infective AdRGD particles were evaluated by the end-point dilution method using 293 cells.

RT-PCR analysis. A549 cells were transfected with each AdRGD at an MOI (multiplicity of infection; $TCID_{50}$/cell) of 50 for 2 h, and then the cells were washed twice with phosphate-buffered saline (PBS) and cultured for 24 h. The expression of mouse chemokine mRNA in these A549 cells was confirmed by an RT-PCR analysis as follows: total RNA was isolated from transduced A549 cells using Sepasol-RNA I Super (Nacalai Tesque, Kyoto, Japan) according to the manufacturer's instructions, following which RT proceeded for 60 min at 42 °C in a 50-μl reaction mixture containing 5 μg total RNA treated with DNase I, 10 μl of 5× RT buffer, 5 mM $MgCl_2$, 1 mM dNTP mix, 1 μM random hexamers, 1 μM oligo(dT), and 100 U ReverTra Ace (Toyobo, Osaka, Japan). PCR amplification of each mouse chemokine and human β-actin transcripts was performed in 50 μl of a reaction mixture containing 1 μl of RT-material, 5 μl of 10× PCR buffer, 1.25 U *Taq* DNA polymerase (Toyobo), 1.5 mM $MgCl_2$, 0.2 mM dNTP, and 0.4 μM primers. The sequences of the specific primers used for PCR amplification and the expected PCR product sizes are defined in Table 1. After denaturation for 2 min at 95 °C, 30 (mouse chemokine) or 20 (human β-actin) cycles of denaturation for 30 s at 95 °C, annealing for 30 s at 55 °C (human β-actin), 60 °C (mouse CCL17, CCL19, CCL20, CCL22, and CX3CL1), 62 °C (mouse CCL21 and XCL1), or 63 °C (mouse CCL27), and extension for 30 s at 72 °C were repeated and followed by completion for 4 min at 72 °C. The PCR product was electrophoresed on a 3% agarose gel, stained with ethidium bromide, and visualized under ultraviolet radiation. EZ Load (Bio-Rad, Tokyo, Japan) was used as a 100 bp molecular ruler.

In vitro chemotaxis assay. A549 cells were transfected with each AdRGD at an MOI of 50 for 2 h, and then the cells were washed twice with PBS and cultured in media containing 10% FBS. After 24 h

Table 1
Primer sequences used for PCR amplification

Gene	Primer sequence (5′ → 3′)	Product size (bp)
Mouse CCL17	(F) TGC TTC TGG GGA CTT TTC TG (R) CCT TGG GTT TTT CAC CAA TC	242
Mouse CCL19	(F) GAA AGC CTT CCG CTA CCT TC (R) TGC TGT TGC CTT TGT TCT TG	164
Mouse CCL20	(F) CGA CTG TTG CCT CTC GTA CA (R) CAC CCA GTT CTG CTT TGG AT	157
Mouse CCL21	(F) CTG AGC CTC CTT AGC CTG GT (R) TCC TCT TGA GGG CTG TGT CT	381
Mouse CCL22	(F) TAT GGT GCC AAT GTG GAA GA (R) GCA GGA TTT TGA GGT CCA GA	102
Mouse CCL27	(F) CTC CCG CTG TTA CTG TTG CT (R) AGT TTT GCT GTT GGG GGT TT	331
Mouse XCL1	(F) ATG GGT TGT GGA AGG TGT G (R) GGG AAC AGT TTC AGC CAT GT	250
Mouse CX3CL1	(F) GCA GTG ACC GGA TCA TCT CT (R) GGC ACC AGG ACG TAT GAG TT	701
Human β-actin	(F) CCT TCC TGG GCA TGG AGT CCT G (R) GGA GCA ATG ATC TTG ATC TTC	202

cultivation, cells were washed and incubated with an assay medium (phenol red-free RPMI 1640 containing 0.5% bovine serum albumin and 20 mM Hepes, pH 7.4) for another 24 h. The resulting conditioned medium was collected, and its chemoattractant activity was measured by an in vitro chemotaxis assay across a polycarbonate membrane with 5-μm pores (Chemotaxicell-24; Kurabo, Osaka, Japan) using L1.2 transfectants expressing the specific receptor for chemokines. Recombinant chemokines corresponding to each specific receptor (mouse: CCL19, CCL20, CCL22, CCL27, XCL1, and CX3CL1) were purchased from DakoCytomation (Kyoto, Japan) and used as a positive control for cell migration. Migration was allowed for 2 h at 37 °C in a 5% CO_2 atmosphere. The migrated cells were lysed and quantitated using a PicoGreen dsDNA quantitation reagent (Invitrogen, Tokyo, Japan), and the migration activity was expressed in term of the percentage of the input cells calculated by the following formula: (% of input cells) = (the number of migrated cells)/(the number of cells placed in Chemotaxicell-24; 1×10^6 cells) × 100.

Evaluation of growth of chemokine gene-transduced tumor cells in immunocompetent mice. B16BL6, CT26, and OV-HM cells were transfected with each AdRGD at an MOI of 400, 50, and 10, respectively. After 24 h cultivation, the cells were harvested and washed three times with PBS, and then 2×10^5 transduced B16BL6 cells, 2×10^5 transduced CT26 cells, and 1×10^6 transduced OV-HM cells were intradermally inoculated into the flank of C57BL/6 mice, BALB/c mice, and B6C3F1 mice, respectively. The major and minor axes of the tumor were measured using microcalipers, and the tumor volume was calculated by the following formula: (tumor volume; mm^3) = (major axis; mm) × (minor axis; mm)^2 × 0.5236 [20]. The mice were euthanized when one of the two measurements was greater than 15 mm. On day 60 after tumor inoculation, the tumor-free mice were judged as individuals that could achieve complete rejection. In some cases, the mice that could completely reject a primary tumor were rechallenged by intradermal injection into the flank with 1×10^6 parental or irrelevant tumor cells without chemokine gene-transduction at 3 months after the initial challenge.

Evaluation of growth and rejection ratio of chemokine gene-transduced B16BL6 cells in mice sensitized with melanoma-associated antigen. The immunization of mice with melanoma-associated antigen was performed by the administration of dendritic cells (DCs) transduced with the gp100 gene. The isolation, cultivation, and gene transduction procedures for C57BL/6 mouse bone marrow-derived DCs conformed to the methods previously described [21]. DCs transfected with Ad-RGD-gp100 at an MOI of 50 for 2 h were intradermally injected into the right flank of C57BL/6 mice at 5×10^5 cells/50 μl. At 1 week after the vaccination, 2×10^5 intact or transduced B16BL6 cells were inoculated into the left flank of the mice. The tumor growth and complete rejection were assessed as described above.

Results

Expression of chemokine mRNA and protein in cells transfected with AdRGD

In order to verify the vector performance of mouse chemokine gene-carried AdRGDs, we first examined

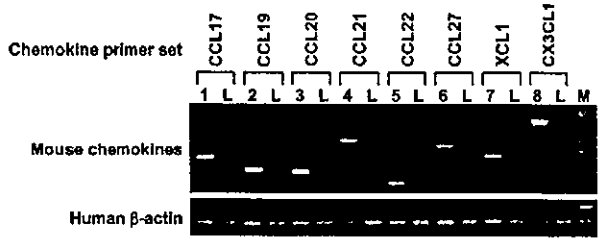

Fig. 1. RT-PCR analysis of chemokine mRNA expression in A549 cells transfected with each chemokine gene-carried AdRGD. PCR for mouse chemokine and human β-actin transcripts was performed on the same RT samples using each specific primer set (summarized in Table 1) to ensure the quality of the procedure. Lane L is negative control using AdRGD-LacZ-transfected A549 (LacZ/A549) cell-derived RT material. Lanes 1–8 represent CCL17/A549, CCL19/A549, CCL20/A549, CCL21/A549, CCL22/A549, CCL27/A549, XCL1/A549, and CX3CL1/A549, respectively. Lane M is a 100 bp molecular ruler.

mRNA expression in transfected cells by an RT-PCR analysis (Fig. 1). In this experiment, human lung carcinoma A549 cells were used instead of murine tumor cells to eliminate the influence of the expression of endogenous mouse chemokine. A549 cells transfected with AdRGD-CCL17, -CCL19, -CCL20, -CCL21, -CCL22, -CCL27, -XCL1, or -CX3CL1 expressed corresponding mouse chemokine mRNA, whereas no PCR products derived from the transcripts of the mouse chemokine gene were detected in AdRGD-LacZ-transfected A549 cells. Next, using in vitro chemotaxis assay, we investigated whether A549 cells transfected with each chemokine gene-carried AdRGD could secrete chemokine protein as a biologically active form into culture supernatants. As shown in Fig. 2, the culture supernatants of each chemokine gene-transduced A549 cell could induce greater migration of cells expressing the corresponding chemokine receptor than those of the intact A549 cells or the AdRGD-Luc-transfected A549 (Luc/A549) cells. The migration of parental L1.2 cells for chemokine receptor-transfectants was not observed in recombinant chemokine-added wells, and they were

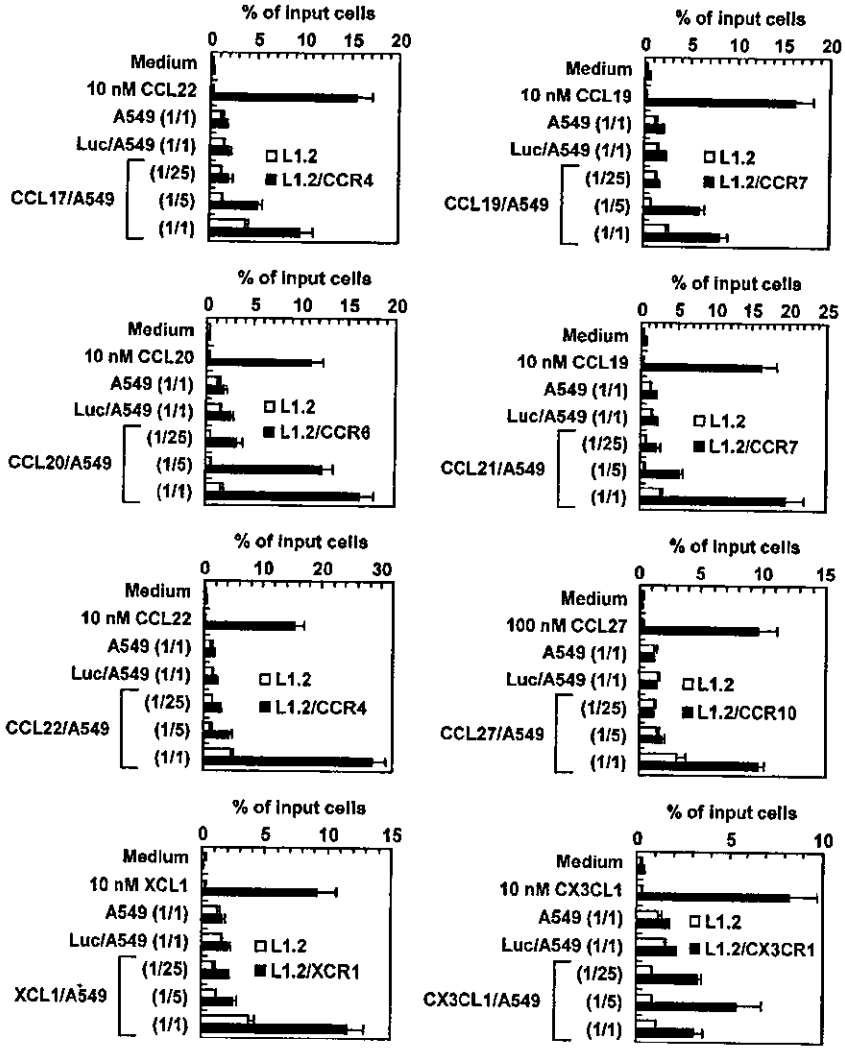

Fig. 2. Chemoattractant activity of culture supernatants of A549 cells transfected with each chemokine gene-carried AdRGD against the stable specific chemokine receptor-expressing cells. The culture supernatants of intact A549 cells, AdRGD-Luc-transfected A549 (Luc/A549) cells, and chemokine gene-transduced A549 cells were prepared and diluted with an assay medium. The fractional values with parentheses in each panel express the dilution factor. These samples and recombinant chemokines dissolved with the assay medium were added to a 24-well culture plate. Cells expressing specific receptors for CCL17 and CCL22 (L1.2/CCR4), CCL20 (L1.2/CCR6), CCL19 and CCL21 (L1.2/CCR7), CCL27 (L1.2/CCR10), XCL1 (L1.2/XCR1), or CX3CL1 (L1.2/CX3CR1) were suspended with the assay medium and placed in a Chemotaxicell-24 installed on each well at 1×10^6 cells. Likewise, parental L1.2 cells for these transfectants were prepared and added to Chemotaxicell-24. Cell migration was allowed for 2 h at 37 °C in a 5% CO_2 atmosphere. The cells that migrated to the lower well were lysed and quantitated using a PicoGreen dsDNA quantitation reagent. The data are expressed as means ± SE of the triplicate results.

maintained at low levels against the culture supernatants of intact A549, Luc/A549, and chemokine gene-transduced A549 cells. These results clearly demonstrated that all AdRGDs encoding each chemokine gene could deliver the concerned gene to target cells, and that transfected cells could secrete the chemokine protein which maintained original chemoattractant activity.

In vivo anti-tumor effect by transfection with chemokine-expressing AdRGD

B16BL6 and CT26 cells were each transfected with eight kinds of chemokine-expressing AdRGDs and AdRGD-Luc, as a control vector, at an MOI of 400 and 50, respectively. OV-HM cells were transfected with

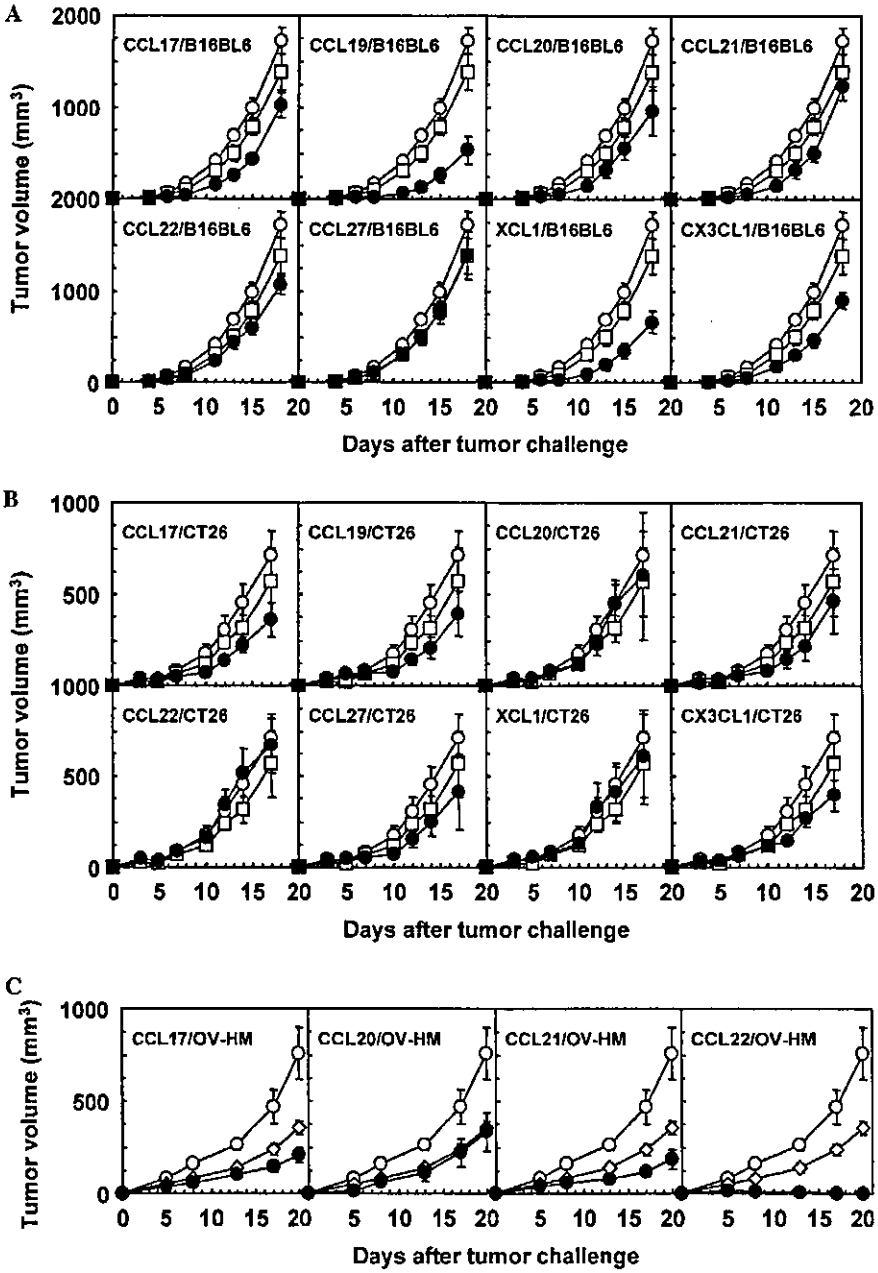

Fig. 3. In vivo growth of three kinds of murine tumor cells transduced with the chemokine gene. B16BL6 cells (A), CT26 cells (B), and OV-HM cells (C) were transfected with each chemokine-expressing AdRGD at an MOI of 400, 50, and 10, respectively, for 24 h. C57BL/6 mice, BALB/c mice, and B6C3F1 mice were intradermally injected in the flank with 2×10^5 transduced B16BL6 cells, 2×10^5 transduced CT26 cells, and 1×10^6 transduced OV-HM cells (●), respectively. Similarly, mice were inoculated with three kinds of intact tumor cells (○), AdRGD-Luc-transfected B16BL6 cells or CT26 cells (□), or AdRGD-Null-transfected OV-HM cells (◇), as control groups. The tumor volume was calculated after measuring the major and minor axes of the tumor at indicated points. Each point represents the mean ± SE of 6–10 mice. The data are representative of two independent experiments.